Reclassification of ankylosaurs with ambiguous taxonomy using tooth morphometrics

Emily G. Cross, Andrew J. Fraass, Terry A. Gates, & Victoria M. Arbour

2026

Original citation:
Cross, E. G., Fraass, A. J., Gates, T. A., & Arbour, V. M. (2026). Reclassification of ankylosaurs with ambiguous taxonomy using tooth morphometrics. *Zoological Journal of the Linnean Society*, *206*(4). https://doi.org/10.1093/zoolinnean/zlag068

Zoological Journal of the Linnean Society, 2026, **206**(**4**), zlag068
https://doi.org/10.1093/zoolinnean/zlag068

OXFORD

Original Article

Reclassification of ankylosaurs with ambiguous taxonomy using tooth morphometrics

Emily G. Cross[1,2,3,*], Andrew J. Fraass[1,4], Terry A. Gates[2,3], Victoria M. Arbour[1,5]

[1]School of Earth and Ocean Sciences, University of Victoria, Victoria, BC V7P 5C2, Canada
[2]Department of Biological Sciences, North Carolina State University, Raleigh, NC 27607, USA
[3]Paleontology, North Carolina Museum of Natural Sciences, Raleigh, NC 27601, USA
[4]Invertebrate Paleontology, The Academy of Natural Sciences of Drexel University, Philadelphia, PA 19103, USA
[5]Department of Natural History, Royal BC Museum, Victoria, BC V8V 9W2, Canada

*Corresponding author. School of Earth and Ocean Sciences, University of Victoria, Victoria, BC V7P 5C2, Canada. E-mail: em.g.cross@gmail.com

ABSTRACT

New morphometric methods of analysis of phylliform ornithischian teeth provide the opportunity to study clade associations of ankylosaurs of ambiguous taxonomy that include dental material. With recent extensive sampling of *ex situ*/*in situ* dentition of ankylosaurs, we present new dental characters for phylogenetic analyses of Thyreophora that we use in seven phylogenetic analyses of both parsimony and Bayesian methods. Our analyses do not recover the previously proposed clades of Panoplosauridae, Polacanthidae, and Struthiosauridae. Prior dental characters that have been used as unambiguous synapomorphies to define Struthiosauridae suffered from vague descriptions that are not accurate portrayals of ankylosaur tooth morphology; therefore, these characters are not useful for thyreophoran phylogenetic analyses. Our phylogenetic analysis results suggest a large degree of homoplasy and support the need for a systematic revision of Nodosauridae. Tooth morphometrics supplement the placement of taxa in phylogenetic analyses and allow clade-level classification of taxa solely or primarily based upon tooth material. We identify clade associations of enigmatic ankylosaur taxa, such as *Peloroplites* with Panoplosauridae, *Aletopelta* with Nodosauridae/Panoplosauridae, and *Priconodon* with Nodosauridae, through a combination of morphometrics and phylogenetics, with implications for palaeobiogeography.

Keywords: morphometrics; phylogenetics; Dinosauria

INTRODUCTION

The phylogenetic and taxonomic utility of ankylosaurian dental traits has been proposed by several authors (Carpenter and Breithaupt 1986, Coombs and Deméré 1996) and recently tested in a quantitative manner by Cross *et al.* (2025). Ankylosaur teeth can be assigned confidently at higher clade levels using linear discriminant analyses of outline shapes, from linear morphometric measurements, and, in some cases, based on absolute size. This success provides the potential to test the clade-level affiliations of several taxa that currently have ambiguous phylogenetic relationships, such as those taxa known only from isolated teeth or fragmentary skeletons. Here, we investigate the clade affiliation of several ankylosaur species with ambiguous taxonomy using traditional and geometric morphometric analyses of their teeth (Table 1).

Dental characters are commonly used in ankylosaur phylogenetic studies (e.g. Thompson *et al.* 2012, Raven *et al.* 2023). We investigate the influence of dental characters on resolving the phylogeny of ankylosaurs, especially in light of recent studies rejecting the long-standing Ankylosauridae–Nodosauridae dichotomy within Ankylosauria that had been accepted for 50 years (Soto-Acuña *et al.* 2021, Raven *et al.* 2023). Raven *et al.* (2023) recovered a novel topology for ankylosaurs consisting of four clades: Ankylosauridae, Panoplosauridae, Polacanthidae, and Struthiosauridae. Soto-Acuña *et al.* (2021) recovered the traditional Nodosauridae and Ankylosauridae, in addition to identifying a new clade that they named Parankylosauria. Based upon the quantified differentiation of ornithischian teeth associated with skulls from Cross *et al.* (2025), we here modify and develop new tooth characters for ankylosaur systematics. We also include

Received 11 December 2025; revised 20 March 2026; accepted 24 March 2026

Table 1. Specimens used in morphometric analyses to test family association.

Taxon	Specimen number	Age	Geological unit	Image source
***Acanthopholis horridus* Huxley, 1867**	BGS GSM 109045[b]	Cenomanian	Lower Chalk	Lomax *et al.* (2014)
***Aletopelta coombsi* Ford & Kirkland, 2001**	*SDSNH 33909*[a] A, *SDSNH 33909*[a] B, *SDSNH 33909*[a] C	Campanian (Coombs and Deméré 1996)	Point Loma Fm	Coombs and Deméré (1996)
***Antarctopelta oliveroi* Salgado & Gasparini, 2006**	*MLP86-X-28-1*[a]A, *MLP86-X-28-1*[a]B	Campanian (Salgado and Gasparini 2006)	Gamma Mbr, Santa Marta Fm	Salgado and Gasparini (2006)
***Borealopelta markmitchelli* Brown *et al.*, 2017**	*TMP2011.033.0001*[a]A, *TMP2011.033.0001*[a]B	Aptian (Brown *et al.* 2017)	Clearwater Fm	C. Brown (pers. comm.)
***Cedarpelta bilbeyhallorum* Carpenter *et al.*, 2001**	*CEUM 1264*[a] #86	Aptian–Albian (Chure *et al.* 2010, Gulbranson *et al.* 2022)	Ruby Ranch Mbr, Cedar Mountain Fm	EGC
***Jakapil kaniukura* Riguetti *et al.*, 2022a**	*MPCA-PV-630*[a] A, *MPCA-PV-630*[a] B, *MPCA-PV-630*[a] C, *MPCA-PV-630*[a] D	Cenomanian (Riguetti *et al.* 2022a)	Candeleros Fm	Riguetti *et al.* (2022a)
***Kunbarrasaurus ieversi* (Leahey *et al.*, 2015), *Minmi* sp. Molnar, 1996**	*QM18101*[a]	Albian (Molnar 1996)	Allaru Mudstone	Molnar (1996)
***Peloroplites cedrimontanus* Carpenter *et al.*, 2008**	*CEUM 34580*[a]	Aptian–Albian (Chure *et al.* 2010, Gulbranson *et al.* 2022)	Ruby Ranch Mbr, Cedar Mountain Fm	EGC
***Priconodon crassus* Marsh, 1888**	USNM 437985 A, USNM 437985 B	Aptian	Arundel Fm	VMA
***Priodontognathus phillipsii* Seeley, 1875**	*CAMSM B5340*[a]	Upper Jurassic (Galton 1980)	Oxford Clay	Lomax *et al.* (2014)
***Sarcolestes leedsi* Lydekker, 1893**	*NHMUK R2682*[a]	Middle Jurassic (Galton 1980)	Oxford Clay	VMA
Sauropelta edwardsorum	AMNH 3016	Valanginian–Cenomanian	Cloverly Fm	Coombs (1990)
	YPM 5350, YPM 5525	Valanginian–Cenomanian	Cloverly Fm	Galton (1980)
***Stegouros elengassen* Soto-Acuña et al., 2021**	*CPAP 3165*[a]	Upper Campanian–Lower Maastrichtian (Soto-Acuña *et al.* 2021)	Dorotea Fm	Soto-Acuña *et al.* (2021)

[a]The specimen is the holotype for a taxon.
[b]The specimen is a syntype.

several recently named thyreophoran taxa that were published after data collection was completed for the study by Raven *et al.* (2023), including the unusual taxa *Stegouros* (Soto-Acuña *et al.*, 2021) and *Jakapil* (Riguetti *et al.* 2022a), to allow for a more complete investigation of thyreophoran relationships.

MATERIALS AND METHODS

Morphometric materials and methods

Cross *et al.* (2025) developed a morphometric dataset of 325 ankylosaur teeth from 35 species. For each taxon in this study, we use the data in the study by Cross *et al.* (2025) or, for new taxa, we follow the morphometric protocol described by Cross *et al.* (2025) to collect new data. For all measurements, we measured crown base lengths (CBL) and crown heights (CH) using digital callipers on the specimens directly when possible or digitally using images on JMorph (Lelièvre and Grey 2017). Outline geometric morphometrics were done on both labial and lingual views of each tooth, when possible, from images in JMorph (Supporting Information, File S1). As in the study by Cross *et al.* (2025), tooth position was not considered, because many ankylosaur skulls do not have enough teeth *in situ* to assess differences in tooth morphology confidently across a tooth row. Additionally, several taxa in the study by Cross *et al.* (2025) and taxa assessed here are *ex situ* teeth associated with skulls and cannot be assigned a tooth position. The ankylosaur taxon *Priconodon*, based solely on teeth, and associated or *in situ* teeth of species with ambiguous taxonomy and those included in Parankylosauria (*sensu* Soto-Acuña *et al.* 2021) are plotted as isolated teeth in principal component analysis (PCA) space to test clade associations based on tooth morphology. Linear discriminant analysis (LDA) classifications and likelihood percentages from multiple classification methods were compared to investigate the consistency of identification. Teeth treated as isolated do not contribute to the construction of the PCA or LDA; instead, they are plotted onto the PCA produced by the teeth associated with other cranial material that allows confident taxonomic assignment. Each PCA space was calculated from a carefully built dataset that did not include any taxa we tested in our taxonomic hypothesis test. Our specific aim is to test the taxonomic association of ankylosaur taxa that are known to be rogue taxa in prior studies for the specific reason that they

contain scant skeletal material, yet all include teeth within their hypodigm.

Taxa of interest

Acanthopholis horridus (Table 1) was named by Huxley (1867) based upon fragmentary material, including several teeth. It has been assigned to Nodosauridae and was not considered in the analyses by Raven *et al.* (2023). Seeley (1869) named several other *Acanthopholis* species; however, all of these are now considered *nomina dubia* (Pereda-Suberbiola and Barrett 1999) of various taxa. *Acanthopholis horridus* is variably considered valid or not valid in systematic reviews (Coombs 1978, Coombs and Maryańska 1990, Pereda-Suberbiola and Barrett 1999). Pereda-Suberbiola and Barrett (1999) consider features of the *Acanthopholis horridus* holotype material consistent with Nodosauridae; however, they note that they are unsure that the teeth alone could be used for a clade-level identification.

Aletopelta coombsi (Table 1) is known from a single specimen, *SDSNH 33909*, preserving primarily the dorsal skeletal section and associated teeth. The clade affiliation of *Aletopelta* has been inconsistent. Coombs and Deméré (1996) suggested that *Aletopelta* is a nodosaurid based upon characteristics of the scapular spine, prespinous fossa, posterior margin of the ilium, and fourth trochanter, but noted that none of the clade-level diagnostic cranial synapomorphies is preserved. Ford and Kirkland (2001) suggested that *Aletopelta* is ankylosaurid based upon characteristics of armour and limb morphology. Its phylogenetic position has changed across different analyses (Vickaryous *et al.* 2004, Thompson *et al.* 2012, Arbour and Currie 2016, Raven *et al.* 2023). Most recent phylogenetic analyses place *Aletopelta* as a nodosaurid or panoplosaurid (Maidment *et al.* 2025, Agnolín *et al.* 2026).

Antarctopelta oliveroi, the ankylosaur from Antarctica, has been identified as a parankylosaurian (Soto-Acuña *et al.* 2024, 2021, Agnolín *et al.* 2026), basal nodosaurid (Thompson *et al.* 2012), indeterminate nodosaurid (Arbour and Currie 2016), polacanthid (Maidment *et al.* 2025), ankylosaurid (Raven *et al.* 2023), and bearer of both ankylosaurid and nodosaurid features (Salgado and Gasparini 2006).

Cedarpelta bilbeyhallorum was originally classified as a shamosaurine-like ankylosaurid (Carpenter *et al.* 2001), but has been classified as ankylosaurid, nodosaurid, and basal ankylosaur in subsequent systematic studies (e.g. Vickaryous *et al.* 2004, Arbour and Currie 2016, Raven *et al.* 2023, respectively). Maidment *et al.* (2025) classified it as an early diverging thyreophoran under equal weights, and as an early diverging ankylosaur with implied weights $k = 3$, where k is the concavity constant. Agnolín *et al.* (2026) recovered *Cedarpelta* as an early diverging ankylosaur in all analyses (equal weights, $k = 3$, $k = 7$, $k = 11$).

Brown *et al.* (2017) indicated that *Borealopelta markmitchelli* is a nodosaurid; however, Raven *et al.* (2023) recovered it as ankylosaurid, noting that its placement might be attributable to its exceptional preservation. Maidment *et al.* (2025) recovered *Borealopelta* as a polacanthid with equal weights and an ankylosaurid with implied weights $k = 3$. Agnolín *et al.* (2026) classified it variably as a nodosaurid and within a large ankylosaur polytomy between different analyses. C. Brown (personal comment, 13 March 2025) provided images of two teeth of the *Borealopelta* holotype (*TMP 2011.033.000*) in labial view with ultraviolet fluorescence.

Jakapil kaniukura is known from a partial skeleton (*MPCA-PV-630*) that includes maxillary and dentary teeth (Riguetti *et al.* 2022a). *Jakapil* contains features of early diverging thyreophorans but is recovered from the Cenomanian and might represent a separate branch of South American thyreophorans (Riguetti *et al.* 2022a). Fonseca *et al.* (2024) found *Jakapil* as either a basal thyreophoran or the basal-most ankylosaur in a comprehensive analysis of ornithischians.

The holotype of *Kunbarrasaurus ieversi* (*QM F18101*) was originally described as *Minmi* sp. (Molnar 1996). Prior to the discovery of *Stegouros* and proposal of the clade Parankylosauria, *Minmi* sp. was considered an ankylosaur, yet not assigned a less inclusive clade (Molnar 1996, Arbour and Currie 2016). Leahey *et al.* (2015) redescribed *QM F18101* as *Kunbarrasaurus ieversi*, supporting the idea that it represents a basal ankylosaur. The description of *Stegouros* suggests that *Kunbarrasaurus* might fit within the Gondwanan thyreophoran clade of Parankylosauria that branches off before the 'nodosaurid–ankylosaurid' dichotomy (Soto-Acuña *et al.* 2021). Recent phylogenetic analyses place *Kunbarrasaurus* in monophyletic Parankylosaria (Agnolín *et al.* 2026). However, Maidment *et al.* (2025) recovered *Kunbarrasaurus* as a nodosaurid (equal weights) and a polacanthid (implied weights $k = 3$). We used one tooth of the holotype *QM F18101* figured by Molnar (1996) to compare the tooth morphology of *Kunbarrasaurus* relative to the other parankylosaurs (Table 1).

Peloroplites cedrimontanus was classified as a polacanthid by Raven *et al.* (2023) and Maidment *et al.* (2025). However, the majority of the characters that are considered synapomorphic for Polacanthidae and Panoplosauridae are missing in *Peloroplites* specimens. Agnolín *et al.* (2026) classified *Peloroplites* as an ankylosaurid (equal weights, $k = 7$, $k = 11$) and as an ankylosaur with no less inclusive clade, across analyses. When the single associated tooth was plotted in the morphospace by Cross *et al.* (2025), it plotted in a location far from the rest of Polacanthidae and had a much larger absolute size than any other polacanthid species.

Priconodon crassus (Table 1) was first described by Marsh (1888) based solely on an isolated tooth. Lull (1911) noted similarity to *Palaeoscincus*, yet assigned it to Stegosauridae. It is typically recognized as an ankylosaur with uncertain clade affinities.

Priodontognathus phillipsii (Table 1) is named based upon a single maxilla fragment (Seeley 1875). It has been identified variously as a stegosaur, an ankylosaur, and a basal thyreophoran (Ősi 2015).

Sarcolestes leedsi is represented by a left maxilla (Lydekker 1893) (Table 1). *Sarcolestes* has historically been included in both Stegosauria and Ankylosauria, although it is currently considered a nodosaurid ankylosaur (Galton 1980, 1983).

Sauropelta edwardsorum has been accepted as a nodosaurid since the study by Coombs (1978). In the study by Raven *et al.* (2023), *Sauropelta* was recovered outside of Ankylosauridae but not within any of the three newly recognized clades representing what were traditionally considered nodosaurids. Maidment *et al.* (2025) classified *Sauropelta* as a nodosaurid (equal weights) and an early diverging ankylosaur (implied weights $k = 3$). Agnolín *et al.* (2026) classified it variably as a nodosaurid (equal weights), an early diverging ankylosaur (implied weights $k = 7$), and an

ankylosaur with no less inclusive clade (implied weights $k = 3$, $k = 11$). We use three teeth of *Sauropelta* (Table 1) to investigate its tooth morphology in comparison to the clades of Raven *et al.* (2023).

Stegouros elengassen is a highly divergent ankylosaur recently described from southern Chile, bearing an independently evolved tail club dissimilar to ankylosaurids and convergent with glyptodonts. Soto-Acuña *et al.* (2021) recovered *Stegouros* along with *Antarctopelta* and *Kunbarrasaurus* to form the new basally diverging clade Parankylosauria. Parankylosauria was supported by a broad ornithischian phylogenetic analysis by Fonseca *et al.* (2024) and further reinforced by Agnolín *et al.* (2026); however, it was not recovered by Maidment *et al.* (2025), with *Stegouros* instead in a basal position in Ankylosauria.

Phylogenetic analyses

We test the effects of some of the diagnostic traits identified by Cross *et al.* (2025) on the interrelationships of ankylosaurs using the phylogenetic dataset developed by Raven *et al.* (2023) by creating new tooth characters and by modifying and removing various characters from Raven *et al.* (2023), because we considered the wording ambiguous and difficult to replicate in coding (Supporting Information, File S2). Specifically, we consider aspects of crown striae and fluting as separate morphological characters, because they are not synonymous; neither the scorings nor character descriptions by Raven *et al.* (2023) accurately represent this distinction. Striae tend to originate from the base or cingulum of the tooth, are often not equidistant, and do not form deep crevice-like structures, whereas fluting tends to originate at the carinae, is often equidistant, and forms larger crevice-like structures (Fig. 1). To reduce ambiguity of crown shape, character 113 in the present character matrix is a modified version of character 114 (tooth crown roundness) of Raven *et al.* (2023), adding a subrounded tooth state: the crown is rounded, but an apex is still discernible. We excluded character 115 (tooth crown height to width comparison) of Raven *et al.* (2023) from the analysis, and we defined two new characters (114 and 115) following the CH and CBL criteria of Cross *et al.* (2025), codifying the occurrence of at least one tooth with a CBL and/or CH of ≥10 mm. We removed character 116 (presence/absence of a central apical ridge) of Raven *et al.* (2023), because these authors indicated that it might be more ecologically correlated, and is yet to be tested. Characters 1–112 are the same as those of Raven *et al.* (2023). Our characters 126–343 are the same as characters [123–340] of Raven *et al.* (2023), only shifted forward three numbers (e.g. Raven *et al.* [123] is our 126).

Additionally, we have coded taxa not present in the study by Raven *et al.* (2023): *Jakapil* (Riguetti *et al.* 2022a), *Stegouros* (Soto-Acuña *et al.* 2021), *Patagopelta* (Riguetti *et al.* 2022b), and an unnamed ankylosaur from Argentina (Álvarez Nogueira *et al.* 2025), for more comprehensive sampling. Furthermore, we were able to score dental characters for species unscored by Raven *et al.* (2023), including *Anodontosaurus*, *Borealopelta*, *Cedarpelta*, *Crichtonpelta*, *Denversaurus*, *Gobisaurus*, and *Jinyunpelta*. We did not score tooth characters for some species included by Raven *et al.* (2023), because there are no published images or descriptions of the teeth, or the illustrations lack fine detail. The species we did not score for dental characters that Raven *et al.* (2023) included are as follows: *Dyoplosaurus*, the Paw Paw juvenile, *Scolosaurus*, and *Tsagantegia*. Additionally, we scored tail characters for *Zuul* that were marked as missing by Raven *et al.* (2023). We do not consider *Tarchia teresae*, *Minotaurasaurus*, and *Zhejiangosaurus* as valid taxa (Arbour and Currie 2016). We include specimen PIN 3142/250, the specimen that Raven *et al.* (2023) scored for *Tarchia teresae* as *Saichania*, and INBR21004, the specimen that Raven *et al.* (2023) scored for *Minotaurasaurus* as *Tarchia kielanae* (Arbour *et al.* 2014).

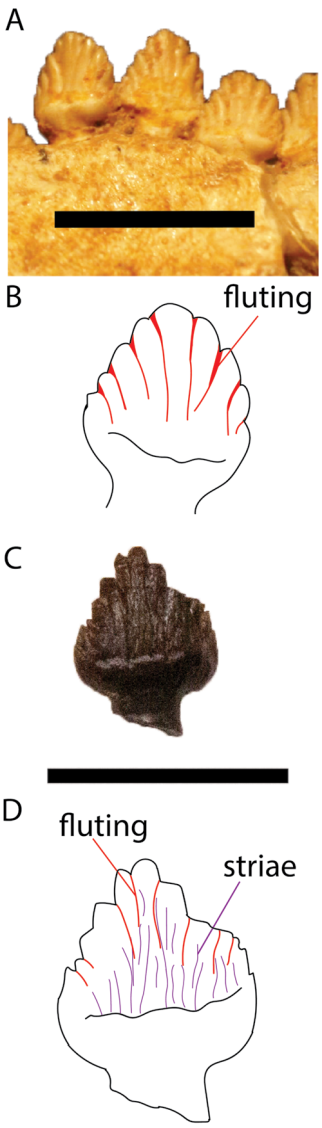

Figure 1. Differences between fluting and striae. A, B, *Pinacosaurus grangeri* (ZPAL MgD II/1) teeth with strong fluting. C, D, *Euoplocephalus tutus* (CMNFV 8876) tooth with minor fluting and striations. Scale bar: 1 cm in A, C.

We perform maximum parsimony and Bayesian inference phylogenetic analyses following methods from Raven *et al.* (2023) to make direct comparisons, and also extend these phylogenetic methodologies to take greater advantage of available data with analytical capabilities (Supporting Information, File S3). All character scoring was completed in Mesquite v.3.81 (Maddison and Maddison 2023). In all analyses, *Lesothosaurus*

is designated as the outgroup. Maximum parsimony trees were constructed in TNT v.1.6 (Goloboff and Morales 2023) using new technology algorithms with 100 random addition sequences and sectorial search, parsimony ratchet with 20 substitutions, tree drifting, and tree fusing with five rounds, as in the study by Raven *et al.* (2023). One thousand trees are held in RAM, and we execute a second round of TBR branch swapping. We identify potential rogue taxa using quick pruning heuristic. The consistency index (CI) and retention index (RI) are calculated using the TNT script STATS.RUN. Total fit and adjusted homoplasy are calculated by TNT. In addition to equal weights, we follow the use of implied weights of Raven *et al.* (2023), with $k = 3$, $k = 8$, and $k = 12$, respectively.

Raven *et al.* (2023) use the R package 'strap' (Bell and Lloyd 2015) to tip date their trees. Studies show that 'strap' uses a less ideal tip dating method than the 'cal3' method or MrBayes tip dating algorithm (Bapst 2014, Bapst and Hopkins 2017). Instead, we used MrBayes (Altekar *et al.* 2004, Ronquist *et al.* 2012) to time scale our parsimony trees, which is similar to 'cal3' methods but is much less likely to create zero-length branches (Matzke and Wright 2016). We add in a 'dummy taxon' that has an age of zero and is adjacent in the tree to *Ankylosaurus*, which has a 'fixed date' at 66.88 Myr. Given that the MrBayes algorithm is designed for tree construction with extant taxa, the dummy taxon ensures that our fixed date taxon is properly dated. We used the functions 'createMrBayesConstraints' and 'createMrBayesTipDatingNexus' from the package 'paleotree' (Bapst 2012) in R v.2023.09.1 + 494 (R Core Team 2021) to convert our trees and occurrence data into a nexus file with MrBayes formatting (Supporting Information, File S3). After Bayesian tree inference, we removed the dummy taxon from the parsimony trees using Mesquite v.3.81 (Maddison and Maddison 2023).

Raven *et al.* (2023) also ran a Bayesian inference tree in MrBayes using the non-clock model with parameters gamma rates, number of gamma categories equal to four, 20 million generations, four runs, eight chains, and a 25% burn-in, which we mimic for analytical comparison. Given that lognormal rate distributions have been shown to approximate discrete morphological character evolution better (Harrison and Larsson 2015), we replaced the gamma rates with lognormal to see whether this modification produced a different topology from the gamma rates. Additionally, we ran a fossilized birth–death clock model that included a dummy taxon coded as all '?' with no time constraints. The clock rate prior was set using the results from a non-clock version of the same taxon–character matrix.

Stratigraphic congruence metrics of all trees were computed using 'StratPhyoCongruence' from the R package 'strap' (Bell and Lloyd 2015). We compared the stratigraphic consistency index (SCI), relative completeness index (RCI), gap excess ratio (GER), and modified Manhattan measure (MSM*) between analyses to determine the most supported tree. Our new characters were mapped onto our preferred tree using 'to.matrix' from the R package 'phytools' (Revell 2024).

Institutional abbreviations

AMNH, American Museum of Natural History, New York, NY, USA; **BGS GSM**, British Geological Survey, Keyworth, Nottingham, UK; **BYU**, Brigham Young University Museum of Paleontology, Provo, UT, USA; **CAMSM**, Sedgwick Museum of Earth Sciences, University of Cambridge, Cambridge, UK; **CEUM**, Utah State University Eastern, Prehistoric Museum, Price, UT, USA; **CMNFV**, Canadian Museum of Nature, Ottawa, ON, Canada; **CPAP**, Colección de Paleobiología de Antártica y Patagonia, Instituto Nacional Antártico Chileno, Punta Arenas, Chile; **DMNH**, Denver Museum of Nature and Science, Denver, CO, USA; **MLP**, Museo de La Plata, Argentina; **MPCA-PV**, Colección de Paleovertebrados de la Museum Provincial de Cipolletti 'Carlos Ameghino', Cipolletti, Rio Negro Province, Argentina; **NHMUK**, Natural History Museum, London, UK; **PIN**, Paleontological Institute, Russian Academy of Sciences, Moscow, Russia; **QM**, Queensland Museum, Geoscience Collection, Brisbane, Queensland, Australia; **ROM**, Royal Ontario Museum, Toronto, ON, Canada; **SMA**, Sauriermuseum Aathal, Switzerland; **SDSNH**, San Diego Natural History Museum, San Diego, CA, USA; **TMP**, Royal Tyrrell Museum of Paleontology, Drumheller, Alberta, Canada; **USNM**, Museum of Natural History, Smithsonian Institution, Washington, DC, USA; **YPM**, Yale Peabody Museum, New Haven, CT, USA; **ZPAL**, Zaklad Paleobiologii (Institute of Paleobiology), Polish Academy of Sciences, Warsaw, Poland.

RESULTS

Tooth morphometrics

Genus-/species-level analysis of individual clades

Plotting individual nodosaurid species (*sensu* Coombs 1978) using the dataset of Cross *et al.* (2025) compares possible morphospace occupation between individual species and genera (Fig. 2). Much of the PCA morphospace is occupied by *Edmontonia rugosidens* (three skulls) (Fig. 2A, C). In PCA labial view, all other nodosaurid species occupy part of the same morphospace as *Edmontonia rugosidens* (Fig. 2A). *Edmontonia rugosidens* is represented by a large number of specimens in comparison to other species in our results using the dataset of Cross *et al.* (2025) at species level and adding new data. The large morphospace spread of *Edmontonia rugosidens* might represent variation between individuals and some heterodonty within individual skulls. Other species represented by multiple individuals (e.g. *Gastonia burgei*) have a smaller spread in PCA morphospace, potentially indicating less dental variability. *Panoplosaurus mirus* and *Edmontonia longiceps* occur entirely within morphospace enclosed by the convex hull of *Edmontonia rugosidens* in the labial view PCA plot (Fig. 2A). The labial view LDA shows considerable overlap between all species (Fig. 2B). *Europelta* (two individuals) has a larger spread in labial LDA space than *Edmontonia rugosidens*, in contrast to their PCA morphospace arrangements (Fig. 2A, B). This finding suggests that *Europelta* has more variation in linear dimensions, thus those dimensions might best be used for differentiating between species in labial view. Interestingly, *Edmontonia* indet. from the Matanuska Formation in Alaska, *Edmontonia longiceps*, and *Animantarx* plot entirely outside of the *Edmontonia rugosidens* morphospace in lingual view. Both species of *Gastonia* plot entirely inside the lingual view PCA morphospace of *Gargoyleosaurus* (Fig. 2C). The lingual view LDA shows separation of *Edmontonia longiceps*, *Animantarx*, *Struthiosaurus languedocensis*, and *Denversaurus* (Fig. 2D).

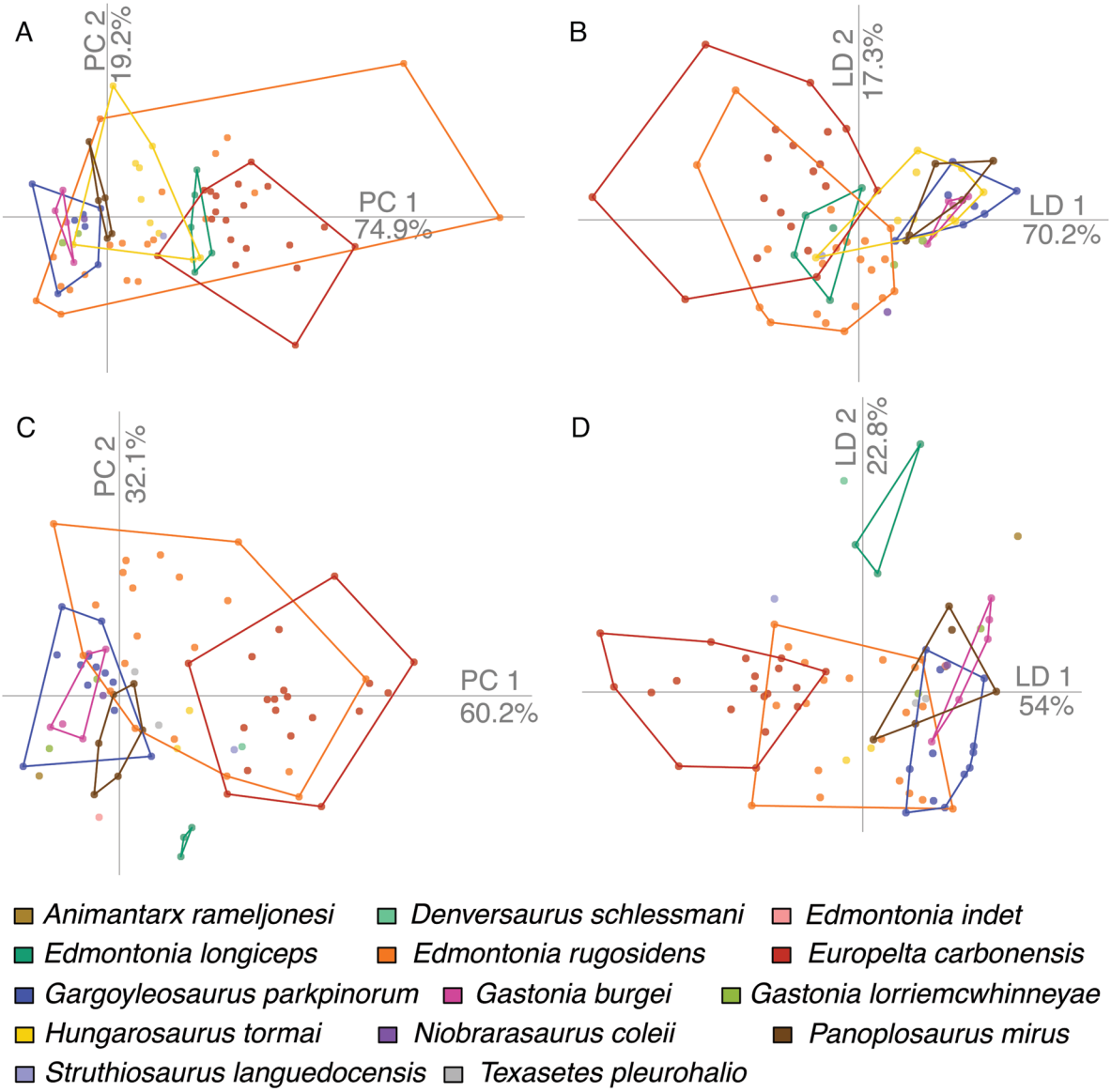

Figure 2. Principal component analyses (PCAs) and linear discriminant analyses (LDAs) of nodosaurid (*sensu* Coombs 1978) phylliform ornithischian teeth at the Coombs (1978) clade level. Labial view: A, PCA; B, LDA. Lingual view: C, PCA; D, LDA.

Ankylosaurid species have less overlap in comparison to the nodosaurid species in labial view and are comparable in overlap in lingual view (Fig. 3). In labial view PCA, the largest morphospace is occupied by *Anodontosaurus* (Fig. 3A). *Tarchia kielanae* falls entirely within the labial PCA morphospace of *Anodontosaurus* (Fig. 3A). Two species, *Liaoningosaurus paradoxus* and *Ankylosaurus magniventris*, plot within morphospace not occupied by other species, for both PCA and LDA, in labial view, whereas the labial LDA shows separation between all ankylosaurid species plotted (Fig. 3A, B). *Liaoningosaurus* is located on the extreme left of principal component (PC) 1, far from all other ankylosaurid species, whereas *Ankylosaurus* is located to the right extreme of PC 1 (Fig. 3A). The lingual PCA shows overlap of most ankylosaurid species (Fig. 3C). *Crichtonpelta benxiensis* has a unique morphospace in comparison to other ankylosaurids in lingual LDA and PCA (Fig. 3C, D). Contrary to the labial view, the lingual view LDA does not completely separate out any species besides *Crichtonpelta*. If geographical location and time are taken into consideration, penecontemporaneous North American taxa have lingual PCA and LDA scores that overlap (e.g. *Anodontosaurus*, *Euoplocephalus*, and *Zuul*), whereas Asian taxa have minimal overlap only in LDA (*Pinacosaurus* and *Saichania*) (Fig. 3C, D). *Ankylosaurus magniventris* is our only Late Maastrichtian North American ankylosaurid representative, and it overlaps in morphology only with *Anodontosaurus* within the ankylosaurid-only lingual LDA (Fig. 3D).

Clade-level analysis of isolated teeth

Several taxa have CH and/or CBL absolute sizes greater than the 10 mm threshold that Cross *et al.* (2025) correlated with a likely nodosaurid identification (*sensu* Coombs 1978). *Aletopelta* has one tooth with a CBL of 9.93 mm and a CH of 9.12 mm, whereas

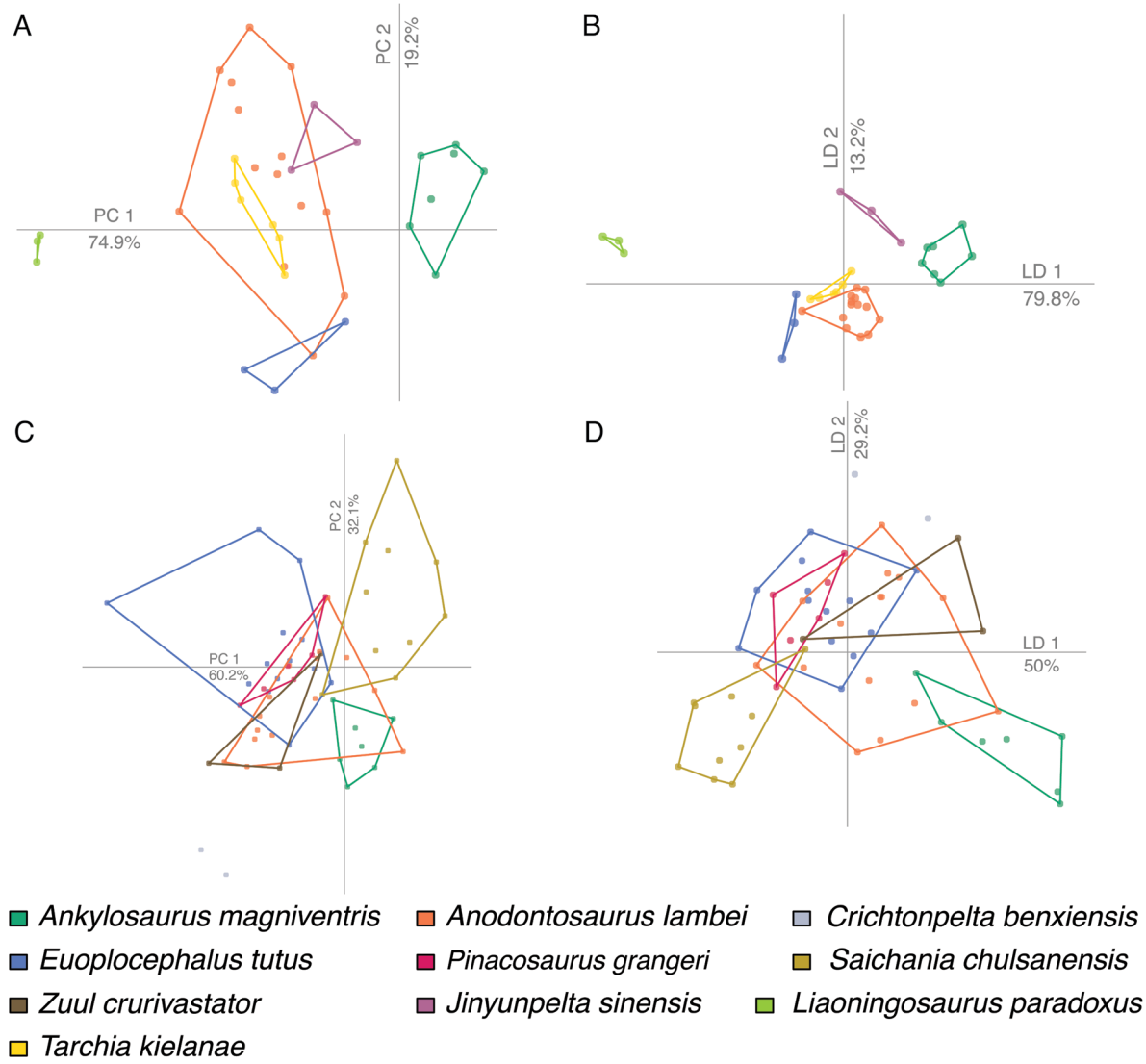

Figure 3. Principal component analyses (PCAs) and linear discriminant analyses (LDAs) of ankylosaurid phylliform ornithischian teeth at the Coombs (1978) clade level. Labial view: A, PCA; B, LDA. Lingual view: C, PCA; D, LDA.

the other two teeth have CBLs and CHs of >11 mm (Table 2). CH and CBL sizes of the two *Antarctopelta* (P 86-X-28-1) teeth approach the 10 mm threshold (Table 2). The holotype of *Cedarpelta* has a single *in situ* tooth (*CEUM 1264* #86), which is not fully erupted, hence we are unable to measure CBL or to carry out an outline analysis. However, the height of the crown is exposed, permitting a CH measurement of 8.49 mm, which is towards the larger side for ankylosaurids and basal ankylosaurs. The single tooth of *Peloroplites* has a CBL of 15.37 mm and a CH of 18.62 mm, placing it well within the range restricted to panoplosaurid nodosaurs in North America. Both teeth of *Priconodon* have high values of CBL and CH (Table 2), identifying them as nodosaurid, panoplosaurid, or struthiosaurid based on size. *Priodontognathus* has a large tooth size, with a CBL of 9.58 mm and a CH of 9.4 mm. Although this value is below the conservative cut-off of 10 mm in size for a definite nodosaurid identification from Cross *et al.* (2025), it approaches the real cut-off from their data (9.4 mm). We assessed one *Sarcolestes* tooth associated with the holotype in labial view. The CBL is 8.48 mm and the CH is 10.83 mm. *Sauropelta* is considered an uncategorized nodosaur by Raven *et al.* (2023). Two *Sauropelta* teeth (YPM 5350 and YPM 5525) have CBL and CH values of >10 mm (Table 2). A third tooth, AMNH 3016, falls below the 10 mm threshold for both CH and CBL.

PCAs and LDAs suggest clade associations with high likelihoods for some of the taxa we assessed (Supporting Information, Files S4 and S5). The analysis of *Aletopelta* by Coombs (1978) provides a nodosaurid identification for two teeth in lingual view (*SDSNH 33909* B and C) and all three teeth in labial view with high likelihoods (Tables 3 and 4). The analysis by Raven *et al.* (2023) provides a panoplosaurid identification for *SDSNH 33909* B in both labial and lingual view with high likelihoods. *SDSNH 33909* A has an ankylosaurid identification with low likelihood in lingual view and a panoplosaurid identification with high likelihood in labial view. *SDSNH 33909* C has lingual and labial identifications as struthiosaurid. When Struthiosauridae is

Table 2. Crown height and crown base length measurements of specimens with ambiguous higher-level taxonomy.

Taxon	Specimen number	CH (mm)	CBL (mm)
Acanthopholis	BGS GSM 109045	9.39	7.39
Aletopelta	*SDSNH 33909* A	9.29	9.91
Aletopelta	*SDSNH 33909* B	11.85	11.22
Aletopelta	*SDSNH 33909* C	12.13	11.50
Antarctopelta	*MLP86-X-28-1*A	10.19	9.46
Antarctopelta	*MLP86-X-28-1*B	8.86	7.48
Cedarpelta	*CEUM 1264 #86*	8.49	
Jakapil	*MPCA-PV-630* A	7.53	5.44
Jakapil	*MPCA-PV-630* B	8.30	5.08
Jakapil	*MPCA-PV-630* C	7.87	5.54
Jakapil	*MPCA-PV-630* D	6.80	4.87
Kunbarrasaurus	*QM18101*	7.77	5.36
Peloroplites	*CEUM 34580*	18.62	15.37
Priconodon	USNM 437985 A	12.54	13.48
Priconodon	USNM 437985 B	15.23	14.08
Priodontognathus	*CAMSM B5340*	9.59	9.41
Sarcolestes	*NHMUK R2682*	10.83	8.48
Sauropelta	AMNH 3016	7.80	7.69
Sauropelta	YPM 5350	12.49	10.69
Sauropelta	YPM 5525	11.60	11.31
Stegouros	*CPAP 3165*	5.42	4.70

Abbreviations: CBL, crown base length; CH, crown height.

removed as an option from the analysis (given the Late Cretaceous Laramidian origin of *Aletopelta* contrasting with the primarily European distribution of known struthiosaurids), *SDSNH 33909* C has a panoplosaurid identification with high likelihood in both views (98% in labial and 95% in lingual). One tooth (*SDSNH 33909* C) falls within morphospace that is occupied only by Panoplosauridae in lingual view (Fig. 4).

Antarctopelta tooth outlines (in both labial and lingual views) plot in the PCA cluster where many of the ornithischian clades overlap in lingual view using the taxonomic frameworks of both Coombs (1978) and Raven *et al.* (2023) (Fig. 4). In labial view, one tooth plots outside of the morphospace for all clades, not near any other teeth treated as isolated in this analysis. In the LDAs, *Antarctopelta* resolves as a thescelosaurid, nodosaurid, or pachycephalosaurid depending on the analysis, and all identifications have <60% likelihood (Tables 3 and 4). Given this inconsistency, no conclusions on *Antarctopelta* systematics can be drawn, other than noting that the one tooth in labial view falls outside the morphospace of other ankylosaur clades, unlike the teeth of the other parankylosaurian, *Stegouros*, suggesting that it might have unique dietary mechanics or feeding ecology.

Jakapil in labial view has inconsistent identifications with low likelihoods (two teeth identified as thescelosaurid, one tooth as ankylosaurid, and one tooth as nodosaurid; Table 3). In lingual view, *MPCA-PV-630* C has a stegosaurid identification with low likelihood (Table 4). In all PCAs, the *Jakapil* teeth cluster in morphospace occupied by multiple clades. The inconsistent low-likelihood identifications of *Jakapil* teeth most probably reflect the highly disparate morphology relative to other thyreophorans represented by this taxon.

Molnar (1996) figures three teeth of *Kunbarrasaurus* (attributed to *Minmi* sp. by Molnar 1996). We analyse one tooth in what we interpret to be labial view (*QM18101*). In LDA, the tooth has an ankylosaurid identification with low likelihood (Table 3), and in the PCAs it plots in morphospace occupied by multiple clades (Fig. 4).

The *Peloroplites* tooth is strongly classified as struthiosaurid or panoplosaurid. The analysis by Coombs (1978) suggests a nodosaurid identification with 91% likelihood (Table 3). Morphometric analysis with all clades of Raven *et al.* (2023) resolves the tooth as struthiosaurid with a 60% likelihood. However, *Peloroplites* is from Cretaceous Laramidia, whereas struthiosaurids are known primarily from Europe. The analysis was completed again without struthiosaurids, and the *Peloroplites* tooth was classified as panoplosaurid with 87% likelihood (Supporting Information, File S5). Notably, *Peloroplites* falls outside of the morphospace of all ankylosaur clades in lingual view PCA space, with the closest clades being Struthiosauridae and Panoplosauridae (Fig. 4).

Using the classification by Coombs (1978), both *Priconodon* teeth are very likely to be nodosaurid (89% and 97%). With the classification by Raven *et al.* (2023), both teeth are identified as likely to be struthiosaurid (97% and 70%). Both *Priconodon* teeth fall strongly in PCA morphospace occupied only by Nodosauridae using the classification by Coombs (1978), and morphospace overlapped by Struthiosauridae and Panoplosauridae with the classification by Raven *et al.* (2023).

The analysis by Coombs (1978) of *Priodontognathus* provides an ankylosaurid identification with 46% likelihood (Table 4). The classification by Raven *et al.* (2023) also suggests an ankylosaurid identification with 76% likelihood. When the *Priodontognathus* isolated tooth is plotted on the PCAs of the associated teeth from Cross *et al.* (2025), it plots in the cluster of all clades (Fig. 4). Given this plot, low LDA likelihoods, and differences in LDA identifications between methods, we suggest that the clade affiliation of *Priodontognathus* remains ambiguous.

Using the classification by Coombs (1978), *Sarcolestes* has a nodosaurid identification with only a 61% likelihood. Using the classification by Raven *et al.* (2023), the tooth has a basal ankylosaur identification with 32% likelihood. Given the Middle Jurassic age, the large size, and the variable identification of nodosaurid and basal ankylosaur, *Sarcolestes* is likely to represent an early nodosaurid or an early diverging ankylosaur.

In labial view, two *Sauropelta* teeth (AMNH 3016 and YPM 5350) have an ankylosaurid identification with low likelihood (Table 3). The third tooth (YPM 5525) has a struthiosaurid identification with low likelihood (60%). In lingual view, AMNH 3016 continues to have a low-likelihood ankylosaurid affiliation, whereas YPM 5350 and YPM 5525 both have weak panoplosaurid identifications (Table 4). With struthiosaurids removed from the analysis based on location, YPM 5525 in labial view has a panoplosaurid identification with high likelihood (93%) and plots in the PCA morphospace only occupied by panoplosaurids (Fig. 4). The other two teeth plot in the PCA morphospace covered by all clades. Given the large tooth sizes paired with YPM 5525 plotting in panoplosaurid-only morphospace, using tooth morphometrics *Sauropelta* should be considered a panoplosaurid nodosaur.

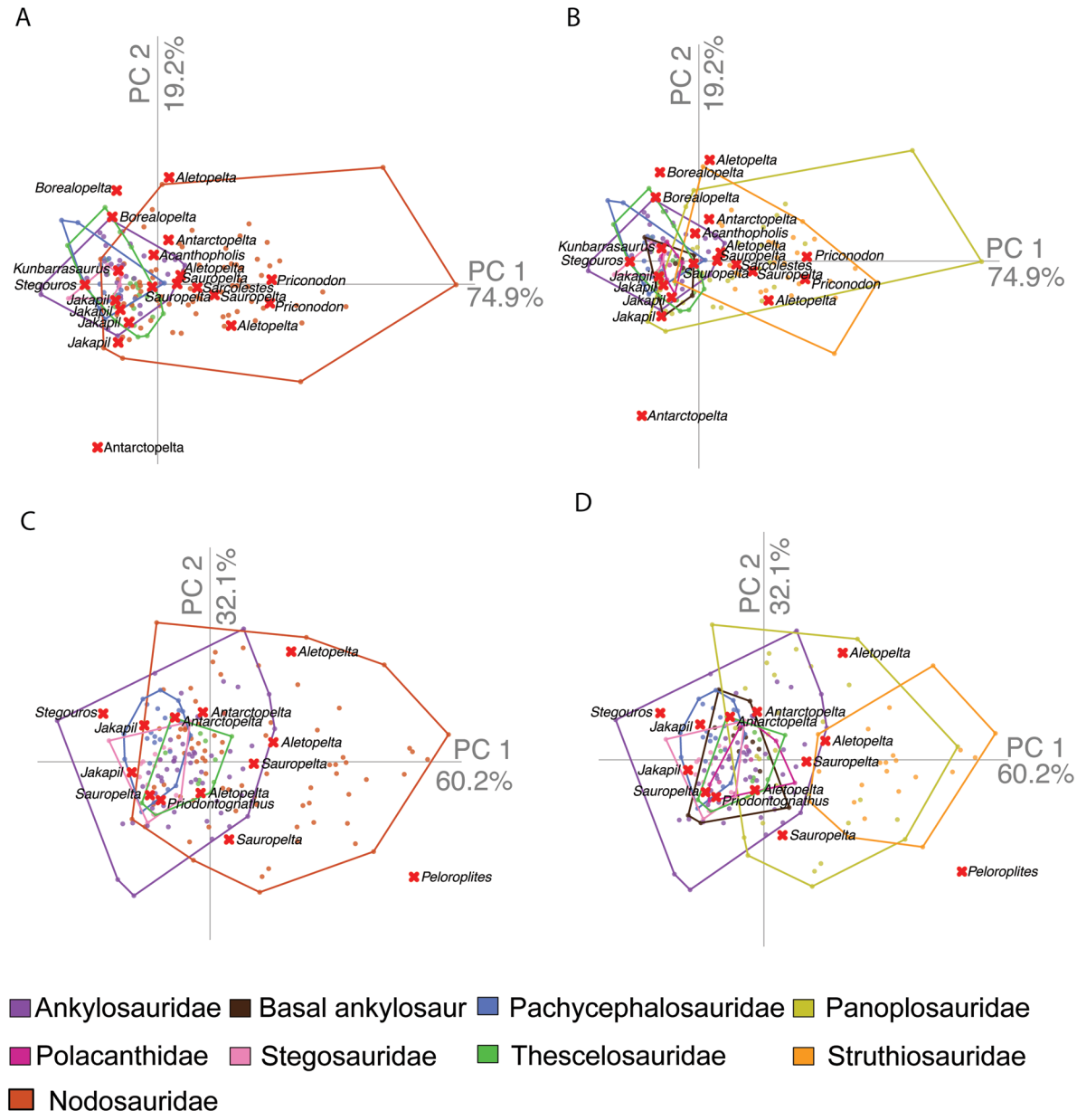

Figure 4. Teeth of ankylosaur species with ambiguous taxonomy plotted in principal component analysis (PCA) space. A, Coombs (1978) clades in labial view. B, Raven *et al.* (2023) clades in labial view. C, Coombs (1978) clades in lingual view. D, Raven *et al.* (2023) clades in lingual view.

In all of the PCA plots in lingual and labial views, *Stegouros* plots on the edge of the morphospace occupied only by Ankylosauridae. Labial view LDA suggests an ankylosaurid identification with low likelihood, whereas lingual view LDA suggests a pachycephalosaurid identification with low likelihood (Tables 3 and 4).

Tree analysis

All tree statistics from each of the parsimony analyses are reported in Table 5 and for the Bayesian analyses in Table 6.

In all of our analyses (both parsimony and Bayesian), we recovered Ankylosauridae and Stegosauria (Figs 5–7; Supporting Information, File S2). Several taxa move around, and yet, the overall clades are retained. Nodosauridae as defined by Coombs (1978) is not recovered or is paraphyletic in all our analyses, except for the Bayesian non-clock analysis (analysis E). Analysis A has the lowest stratigraphic congruence values for nearly every metric, suggesting the lowest performance (Table 5). Analysis C produces our most supported tree using stratigraphic congruence metrics. Parsimony trees have a CI of <.5, and as the implied weights *k* increases, the fit also increases, suggesting high levels of homoplasy.

Within analyses E–G (Bayesian inference), fit is examined through posterior probabilities. Analysis E (non-clock gamma) has no polytomies and recovers both Stegosauria and Ankylosauridae (Supporting Information, File S2). After the run, analysis E reached a standard deviation of 0.0085, and an average

Table 3. Linear discriminant analysis-suggested identifications of teeth of ambiguous taxonomy in labial view.

Taxon	Specimen number	Labial Coombs (1978) clade	Percentage likelihood of Coombs (1978) clade	Labial Raven *et al.* (2023) clade	Percentage likelihood of Raven *et al.* (2023) clade
Acanthopholis	BGS GSM 109045	Ankylosauridae	47.22	Ankylosauridae	52.84
Aletopelta	*SDSNH 33909* A	Nodosauridae	85.87	Panoplosauridae	87.85
Aletopelta	*SDSNH 33909* B	Nodosauridae	50.29	Panoplosauridae	48.18
Aletopelta	*SDSNH 33909* C	Nodosauridae	94.11	Struthiosauridae	81.25
Antarctopelta	*MLP86-X-28-1*A	Nodosauridae	58.26	Panoplosauridae	41.56
Antarctopelta	*MLP86-X-28-1*B	Nodosauridae	54.31	Thescelosauridae	30.68
Borealopelta	*TMP2011.033.0001A*	Ankylosauridae	34.50	Ankylosauridae	31.42
Borealopelta	*TMP2011.033.0001*B	Ankylosauridae	43.14	Ankylosauridae	41.46
Jakapil	*MPCA-PV-630* A	Thescelosauridae	38.06	Thescelosauridae	37.43
Jakapil	*MPCA-PV-630* B	Thescelosauridae	51.97	Thescelosauridae	39.02
Jakapil	*MPCA-PV-630* C	Ankylosauridae	33.30	Ankylosauridae	39.92
Jakapil	*MPCA-PV-630* D	Nodosauridae	55.98	Nodosauridae	36.33
Kunbarrasaurus	*QM18101*	Ankylosauridae	62.01	Ankylosauridae	62.45
Priconodon	USNM 437985 A	Nodosauridae	88.83	Struthiosauridae	97.45
Priconodon	USNM 437985 B	Nodosauridae	97.47	Struthiosauridae	70.38
Sarcolestes	*NHMUK R2682*	Nodosauridae	60.79	Basal ankylosaur	32.16
Sauropelta	AMNH 3016	Ankylosauridae	40.96	Ankylosauridae	46.69
Sauropelta	YPM 5350	Nodosauridae	52.93	Ankylosauridae	42.99
Sauropelta	YPM 5525	Nodosauridae	80.08	Struthiosauridae	56.93
Stegouros	*CPAP 3165*	Ankylosauridae	31.11	Ankylosauridae	30.47

Table 4. Linear discriminant analysis-suggested identifications of teeth of ambiguous taxonomy in lingual view.

Taxon	Specimen number	Lingual Coombs (1978) clade	Percentage likelihood of Coombs (1978) clade	Lingual Raven *et al.* (2023) clade	Percentage likelihood of Raven *et al.* (2023) clade
Aletopelta	*SDSNH 33909* A	Ankylosauridae	54.25	Ankylosauridae	51.85
Aletopelta	*SDSNH 33909* B	Nodosauridae	79.30	Panoplosauridae	61.72
Aletopelta	*SDSNH 33909* C	Nodosauridae	87.25	Struthiosauridae	77.25
Antarctopelta	*MLP86-X-28-1*A	Pachycephalosauridae	31.87	Thescelosauridae	43.85
Antarctopelta	*MLP86-X-28-1*B	Pachycephalosauridae	40.91	Pachycephalosauridae	38.57
Jakapil	*MPCA-PV-630* C	Stegosauridae	61.56	Stegosauridae	78.17
Peloroplites	*CEUM 34580*	Nodosauridae	90.65	Struthiosauridae	60.16
Priodontognathus	*CAMSM B5340*	Ankylosauridae	46.06	Ankylosauridae	52.49
Sauropelta	AMNH 3016	Ankylosauridae	54.24	Ankylosauridae	51.85
Sauropelta	YPM 5350	Nodosauridae	52.40	Panoplosauridae	62.97
Sauropelta	YPM 5525	Nodosauridae	74.15	Panoplosauridae	36.07
Stegouros	*CPAP 3165*	Pachycephalosauridae	72.15	Pachycephalosauridae	38.57

Table 5. Parsimony analysis parameters, resulting analysis metrics, and stratigraphic congruence values.

Analysis	Parameters	Trees retained	Fit	Adjusted homoplasy	CI	RI	SCI	RCI	GER	MSM*
A	Equal weights	6	156.592	186.408	.190	.239	.370	−175.940	.687	.055
B	Implied weights ($k=3$)	6	180.285	162.715	.232	.409	**.568**	−86.260	.795	.082
C	Implied weights ($k=8$)	19	243.189	99.811	.231	.406	.493	**−75.631**	**.808**	**.087**
D	Implied weights ($k=12$)	8	269.283	73.717	.240	.434	.560	−175.720	.688	.055

Highest values are in bold.
Abbreviations: CI, consistency index; GER, gap excess ratio; MSM*, modified Manhattan stratigraphic measure; RCI, relative completeness index; RI, retention index; SCI, stratigraphic consistency index.

Table 6. Bayesian analysis parameters and resulting analysis metrics.

Analysis	Clock type	Rate parameters	Rate category	Clock parameters	Clock rate prior	Clock rate variation	Tree age prior
E	Non-clock	Gamma	4	NA	NA	NA	offsetexp(201.3-215)
F	Non-clock	Lognormal	NA	NA	NA	NA	offsetexp(201.3-215)
G	Fossilized birth–death	Gamma	4	Speciation = exp(1); extinction = beta(1,1); fossilization = beta(1,1); sampling = 0.0000000000001	lognorm(−2.23, 1.11)	TK02; TK02varpr=exp(1)	offsetexp(201.3-215)

NA, Not Applicable.

effective sample size of 5690.42 for tree length and 5297.95 for rate (alpha). Analysis E recovers a monophyletic Nodosauridae. Analysis F (lognormal non-clock) has the same outcomes as analysis E, with a standard deviation of 0.0085, and an average effective sample size of 5690.42 for tree length and 5297.95 for rate (alpha) (Supporting Information, File S2). Analysis G (clock gamma) has large polytomies; however, there are still clades representing Stegosauria and Ankylosaurinae (Supporting Information, File S2). Analysis G reached a standard deviation of 0.00999 (upon which time we stopped the analysis), with a tree length average effective sample size of 107.83, tree height 109.14, and alpha 3353.80. All the metrics for analysis G reached convergence except for TK02 variation (effective sample size of 90.49). The analysis G clock tree is plotted on the geological time scale using the median root age of 228.6 Mya. Stratigraphic congruence metrics for analysis G include SCI = .333, RCI = −404.335, GER = .413, and MSM* = .030.

DISCUSSION

Phylogenetic topologies recovered from parsimony or Bayesian analyses are the result of both the data input and the model parameters set by the researchers. Constant additions and modifications to analyses are essential to reach consensus of both alpha and higher-level taxonomic stability. We applied results from the largest morphometric dataset of thyreophoran and basal ornithischian teeth to modify phylogenetic characters of the most recent and largest thyreophoran character matrix (Raven *et al.* 2023). Results from our study weigh heavily into the discussion of clade-level taxonomy and species-level evolutionary relationships.

Higher-level taxonomy

As noted above, Raven *et al.* (2023) proposed a new four-clade taxonomy for Ankylosauria, eliminating the prior dichotomous clade taxonomy. These authors included two dental characters as unambiguous synapomorphies used to define Struthiosauridae: character 114, subtriangular shape of the tooth crown; and character 118, striations not extending to the cingulum. We modified character 114 to include an intermediate character state of sub-rounded, because the crown can be rounded with a still discernible crown apex (character 113 in this study). We scored one taxon (*Struthiosaurus austriacus*), included within Struthiosauridae by Raven *et al.* (2023), as having a shape different from sub-triangular and 30 taxa not included in Struthiosauridae as having a sub-triangular shape. In our character matrix, we completely changed the second dental character that Raven *et al.* (2023) used to define Struthiosauridae. These authors did not discriminate between striations and fluting, using the term 'striations' while describing 'fluting', resulting in inconsistent scoring. We separate characters related to striations and fluting, with 10 non-'struthiosaurid' taxa having scores for the extent of fluting and/or striations not extending across the full crown. As such, the two dental characters that Raven *et al.* (2023) used as unambiguous struthiosaurid synapomorphies do not accurately assess thyreophoran tooth morphology or taxonomy.

With the changes to nine dental characters in the matrix, only one of our five analyses recovered a topology similar to the preferred tree structure of Raven *et al.* (2023), although with key differences (Fig. 6). Analysis B resolves the Stegosauria clade, with the inclusion of *Invictarx*. Importantly, analysis B is the only consensus tree that resolves *Borealopelta* within Ankylosauridae, as in the study by Raven *et al.* (2023). We do recover a clade with the same members of Panoplosauridae as Raven *et al.* (2023), although our Panoplosauridae has the addition of *Aletopelta* (an ankylosaurid in the study by Raven *et al.* 2023), and the relationships amongst species differ between our topology and the latter authors. Likwise, we recover clades of 'struthiosaurids' and 'polacanthids', although the constituents of these groups differ. Raven *et al.* (2023) defined Struthiosauridae as 'all ankylosaurs more closely related to *Struthiosaurus austriacus* than to *Ankylosaurus*, *Panoplosaurus*, or *Gastonia burgei*' (p. 18). We do recover a clade that matches this description, although it contains 10 additional taxa not present in the Struthiosauridae of Raven *et al.* (2023). It is likely that our revision of the dental characters mentioned above contributes to these changes. Raven *et al.* (2023) defined Polacanthidae as 'all ankylosaurs more closely related to *Gastonia burgei* than to *Ankylosaurus*, *Panoplosaurus*, or *Struthiosaurus austriacus*' (p. 18). In our analysis B, *Gastonia burgei* is in a different clade to *Polacanthus*, with *Polacanthus* being more closely related to *Struthiosaurus austriacus*, and with the two species of *Gastonia* occurring at the base of Ankylosauridae. Using the definitions of Raven *et al.* (2023), Polacanthidae is not recovered in analysis B.

Overall, the increase in total fit values with increases in implied weights shows that there is a large amount of homoplasy in the character matrix used in this study. Analysis A (equal weights) here has a large polytomy within Ankylosauria (Fig. 5). There is a clear Ankylosauridae branch, but no nodosaurid (*sensu* Coombs 1978) or stegosaur clades are resolved. The large polytomy suggests that more work is needed on basal and nodosaurid (*sensu* Coombs 1978) species to investigate whether an ankylosaur dichotomy is realistic. Analysis C (implied weights $k = 8$) has a topology different from both those of Coombs (1978) and Raven *et al.* (2023), with two main nodosaurid clades (Fig. 7). Both nodosaurid clades contain species from all Raven *et al.* (2023) nodosaurid clades and are characterized by large polytomies. Raven *et al.* (2023) found their implied weights $k = 3$ tree to be the most supported through stratigraphic congruence metrics; however, we find analysis C (implied weights $k = 8$) to be the tree with the most support in our analyses. Analysis D (implied weights $k = 12$) has nearly all nodosaurid species (*sensu* Coombs 1978) in a large polytomy. Although we have attempted to focus purely on clades here, if considering only the rigid taxonomic hierarchy, Ankylosauridae is the only resolved ankylosaur family in analysis D. Analysis G (Bayesian inference, fossilized birth–death model) contains a large polytomy within Ankylosauria. Much of the ankylosaur material scored in the matrix of Raven *et al.* (2023) is incomplete and therefore scored as 'missing'. The large amount of missing data contributes heavily to the polytomies in the Bayesian analysis. Further work revising other skeletal characters and reducing the inclusion of largely incomplete taxa might provide resolution in Bayesian analyses.

We mapped our characters 113–120 on our most supported tree (tree C) to understand the homoplasticity of tooth characters (Supporting Information, File S2K–R). Characters 114–115 seem to have a non-random phylogenetic signal. Character 113 is homoplastic across the tree (Supporting Information, File S2K), suggesting that overall tooth shape should be assessed with geometric morphometrics, which can identify subtler and continuous differences in tooth shape between clades. Striation and fluting characters are also homoplastic (characters 117, 119, and 120) (Supporting Information, File S2O, Q, R), which is consistent with the outcomes of Cross *et al.* (2025) on fluting. State 1 (fluting non-confluent with denticles) of character 118 is present in only two taxa in the tree: an early diverging ornithischian (*Laquintasaura*) and a nodosaur (*sensu* Coombs 1978) (*Panoplosaurus*) (Supporting Information, File S2P). Character 114 (at least one tooth CBL > 10mm) shows less homoplasy, present only in nodosaurids (one clade) and a few stegosaurs (Supporting Information, File S2L). There are no ankylosaurids with this trait. The large amount of evolutionary time separating the stegosaurs and nodosaurs with at least one tooth with CBL > 10 mm suggests that these two groups independently derived large CBLs. Character 115 (CH) is more homoplastic than CBL (Supporting Information, File S2M). *Sarcolestes* appears at the base of Ankylosauridae in our tree; however, this taxon is very incomplete, known from only a single left mandible. The scoring of character 115 of the *Sarcolestes* maxillary tooth suggests a likely nodosaurid identification. The only 'ankylosaurid tooth' that scored with a CBL > 10 mm for character 115 is the shamosaurine *Gobisaurus*, with ankylosaurines scoring only zero or missing. As with character 114, the large amount of time and nodes between transitions to state 1 suggest independent derivations of this character state.

Through all of our analyses, we obtained only a single tree that had some similarity to the preferred tree of Raven *et al.* (2023), thus suggesting substantially lower confidence in their four-clade system, especially given that they become unresolved with modifications to only a few dental characters and three additional taxa. Our new and modified tooth characters and time scaling in MrBayes rather than the R package 'strap' (Bell and Lloyd 2015; as in the study by Raven *et al.* 2023) contribute to the recovery of higher stratigraphic congruence metric values for our two most supported trees (analyses B and C) than Raven *et al.* (2023) recovered from any of their trees.

The consistent polytomies of nodosaurs between our analyses supports the idea that Nodosauridae (*sensu* Coombs 1978) need a systematic revision. There has been limited systematic work on Nodosauridae in comparison to Ankylosauridae, the latter of which has had several alpha-taxonomic revisions in recent years (e.g. Arbour and Currie 2013, 2016, Arbour *et al.* 2014). As highlighted earlier, there are many nodosaurid species (*sensu* Coombs 1978) that should be re-evaluated for synonymy or over-lumping, such as the large variation in *Edmontonia rugosidens* (see below). Although many interesting and well-preserved nodosaurid species have been described over the past decade, much of the North American 'mid'-Cretaceous material has not been reassessed in light of these newly described taxa since the work by Carpenter and Kirkland (1998). Phylogenetic analyses of all ankylosaur

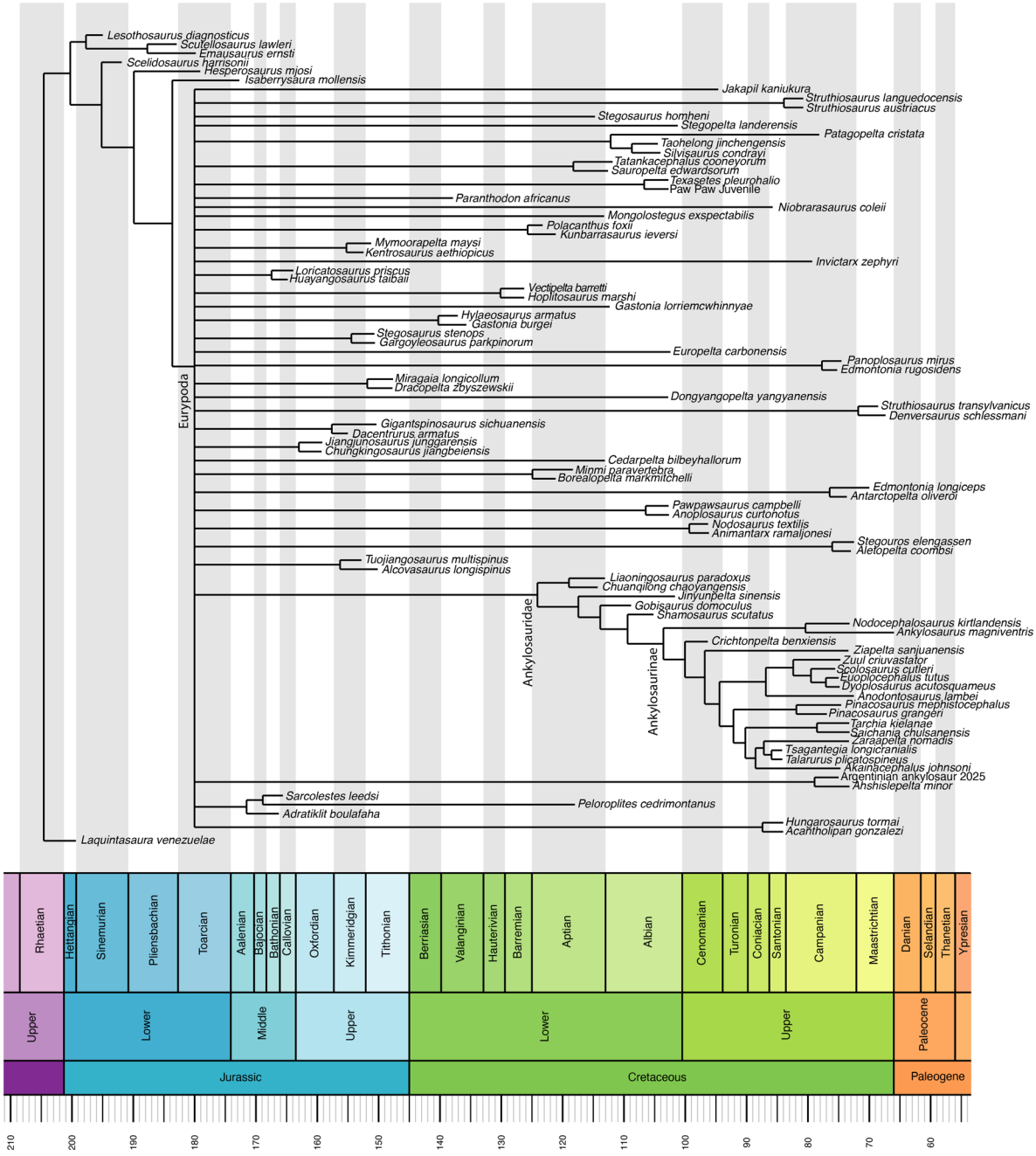

Figure 5. Analysis A (equal weights) strict consensus tree.

clades would be undertaken most effectively only once an alpha-taxonomic level revision of Nodosauridae has been completed.

None of our phylogenetic analyses was able to resolve the other new ankylosaurian clade proposed recently, Parankylosauria (Soto-Acuña *et al.* 2021). Soto-Acuña *et al.* describe Parankylosauria as including 'the first ancestor of *Stegouros*—but not *Ankylosaurus*—and all descendants of that ancestor' (p. 262), yet all of our analyses place *Stegouros* within Ankylosauria. The closest results we received were analyses B and D, proposing *Antarctopelta* and *Stegouros* as sister taxa. Raven *et al.* (2023) did not include *Stegorous* and did not resolve a clade similar to Soto-Acuna's Parankylosauria. Maidment *et al.* (2025) added *Stegouros* to the matrix of Raven *et al.* (2023) and did not recover Parankylosauria. Additional characters related to tail weaponry might be able to provide better resolution; however, that is beyond the scope of the present work. The paper by Agnolín *et al.* (2026), which was published while the present manuscript was in review, added 24 new characters from the Raven *et al.* (2023) matrix that they indicate are present and important for Parankylosauria, in addition to modifying the scorings for several parankylosaurian elements. Agnolín *et al.* (2026) added one tooth character relating to whether the basal cingulum is smooth or crenulate from fluting. As we observed, fluting traits are homoplastic between

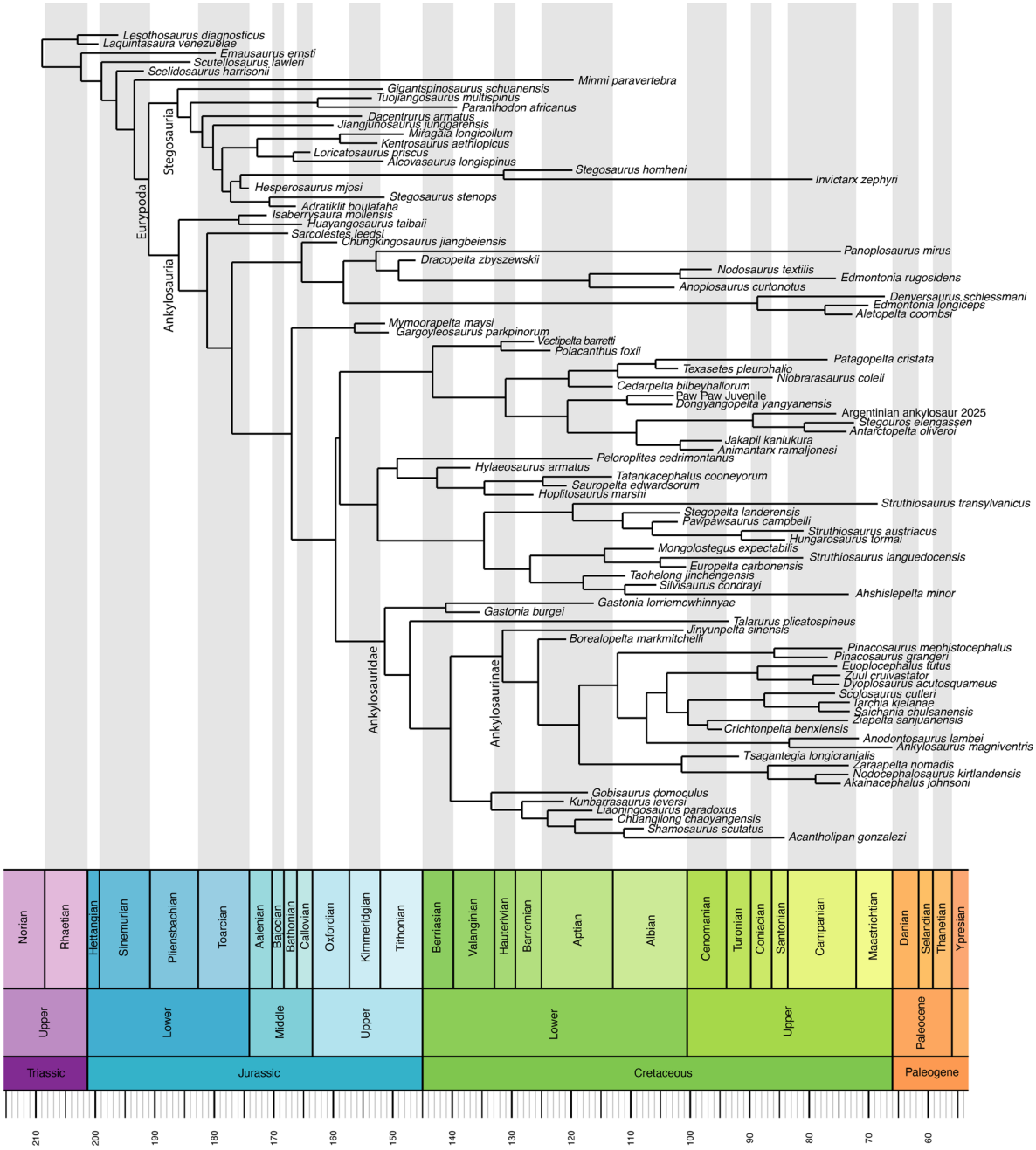

Figure 6. Analysis B (implied weights $k = 3$) strict consensus tree.

thyreophoran groups, and this is likely to be a non-informative character. With these additional characters and modified scorings, Agnolín *et al.* (2026) recovered Parankylosauria as a clade in multiple phylogenetic analyses. It is unsurprising that Parankylosauria does not resolve in our study, because the data we used were only a modification of tooth characters in the analysis by Raven *et al.* (2023), and we find no tooth characters unique to Parankylosauria.

Isaberrysaura + *Huayangosaurus* is recovered in the majority of our analyses but is unusually placed within Ankylosauria. *Huayangosaurus* is described as an early diverging stegosaur, not displaying four of the synapomorphies that unite the rest of the stegosaurs (Sereno and Zhimin 1992). *Isaberrysaura* is known from a relatively incomplete holotype specimen (only 5.9% completeness score in the study by Raven *et al.* 2023), but displays 27 synapomorphies with *Huayangosaurus* (Raven *et al.* 2023). Raven *et al.* (2023) recovered *Isaberrysaura* + *Huayangosaurus* as a clade within Stegosauria. Our analyses B–D also recover this clade. However, analyses B ($k = 3$) and C (preferred tree $k = 8$) place this clade within Ankylosauria after time scaling. Prior to time scaling, this clade is in a large polytomy within Eurypoda (Supporting Information, File S2D, E). Agnolín *et al.* (2026) recovered *Isaberrysaura* and *Huayangosaurus* within a large Eurypoda

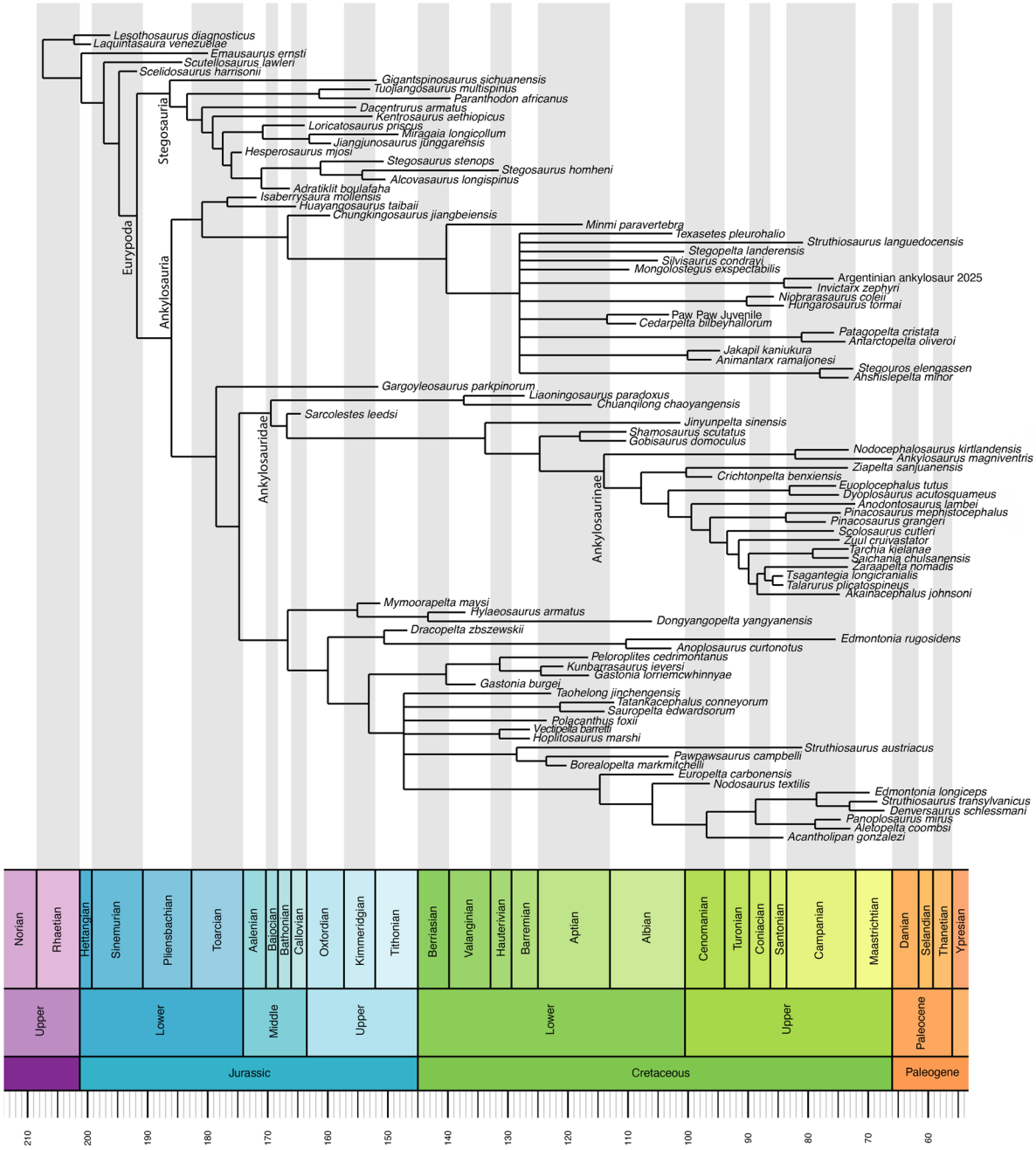

Figure 7. Preferred tree from analysis C (implied weights $k = 8$).

polytomy with equal rates, although when pruning unstable taxa, it places *Isaberrysaura* and *Huayangosaurus* at the base of Stegosauria. With implied weights $k = 3$, Agnolín *et al.* (2026) recover two large clades within Stegosauria, and the clade of *Isaberrysaura* + *Huayangosaurus* is within a clade containing *Gigantspinosaurus*, *Chungkingosaurus*, and *Tuojiangosaurus*. The clade of *Isaberrysaura* + *Huayangosaurus* is at the base of Stegosauria in the study by Agnolín *et al.* (2026) with $k = 7$ and $k = 11$. As outlined above, *Isaberrysaurus* and *Huayangosaurus* appear to be unstable taxa when comparing different phylogenetic analyses. Our unusual placement of this clade within Ankylosauria is probably attributable to the 'primitiveness' of *Huayangosaurus* + *Isaberrysaura* and thus analyses not pulling their grouping into Stegosauria within the non-time-scaled trees, and or the MrBayes time-scaling methodology.

Lower-level taxonomy

Nodosaurid tooth morphometric data plot over a wide PCA space, and much of this variation is occupied by the genus *Edmontonia*, particularly *Edmontonia rugosidens*. Our data include 54 *Edmontonia* teeth, 44 from *Edmontonia rugosidens*, 9 from *Edmontonia longiceps*, and 1 from *Edmontonia* indet. As a point of comparison to contextualize the scale of this variation, the dispecific genus *Gastonia* (represented by 13 teeth of the two species)

displays less variation than that observed in *Edmontonia*. Numerous authors, such as Carpenter (1990) and Burns (2015), have noted that *Edmontonia* is in need of a revision. Raven *et al.* (2023) found *Edmontonia* to be paraphyletic and suggested that additional work is needed to resolve the phylogeny and taxonomy of species within Panoplosauridae. Specifically, they found *Edmontonia longiceps* and *Edmontonia rugosidens* as species with relative completeness of known material, but somewhat unstable in classification, indicating variation in traits between specimens identified as the same species and suggesting the need for further descriptive work. Additionally, *Edmontonia* has a large geographical and temporal range with respect to other ankylosaurs (Vickaryous *et al.* 2004). Given how much morphological, geographical, and temporal variation in Nodosauridae is covered by *Edmontonia* (Fig. 2), this research supports the call for the re-evaluation of *Edmontonia*.

There are a handful of taxa within Ankylosauria that switch between clades among phylogenetic analyses in different studies, but our morphometric and phylogenetic data provide evidence towards clade-level identifications. *Aletopelta* has been interpreted variously as both a nodosaurid and ankylosaurid ankylosaur. The teeth of *Aletopelta* consistently plot within the size and morphospace ranges for nodosaurids/panoplosaurids (Fig. 4). Given the absolute tooth sizes, LDA likelihoods, and PCA plots, it is strongly plausible that *Aletopleta* is a nodosaurid/panoplosaurid. Additionally, *Aletopelta* does not plot within Ankylosauridae in any of our phylogenetic analyses. The only known specimen of *Aletopelta* is sourced from marine sediments in California, USA (Coombs and Deméré 1996). A nodosaurid identity for *Aletopelta* strengthens the previously identified positive association of nodosaurids in marine formations compared to ankylosaurids (Arbour *et al.* 2016, Cross *et al.* 2025), supporting different ecological preferences.

All of our trees (except analysis B), place *Borealopelta* as a nodosaurid, disagreeing with the 'ankylosaurid' classification from Raven *et al.* (2023). Although the teeth of *Borealopelta* were not figured in the original description, we were able to acquire photographs of the teeth for this project, allowing us to score these in a phylogenetic matrix for the first time. We recovered *Borealopelta* within the nodosaurids, which is more consistent with many of its anatomical features, and as it was originally recovered by Brown *et al.* (2017). This indicates that the inclusion of dental characters is important for thyreophoran systematics. The inclusion of *Borealopelta* in Nodosauridae (*sensu* Coombs 1978) further supports the hypothesis by Arbour *et al.* (2016) of nodosaurid–marine formation associations.

The three parankylosaur species investigated here for tooth morphology (*Antarctopelta*, *Kunbarrasaurus*, and *Stegouros*) occupied different regions of PCA morphospace in our morphometric analyses. One tooth of *Antarctopelta* plotted within the cluster of multiple leaf-shaped ornithischian clades, whereas the other tooth plotted outside of the occupied morphospace from the associated data from Cross *et al.* (2025) in labial view. Prior to the discovery of *Stegouros* and the identification of Parankylosauria, *Antarctopelta* was sometimes recovered as a nodosaurid (Thompson *et al.* 2012, Arbour and Currie 2016) or sometimes ankylosaurid (Salgado and Gasparini 2006, Raven *et al.* 2023). *Kunbarrasaurus* also plotted in the cluster of multiple ornithischian clades, close to the tooth of *Stegouros*. All parankylosaurian teeth, other than one *Antarctopelta* tooth in labial view, plot in morphospace occupied by other clades, suggesting that their teeth are also not distinct in morphology. The CH and CBL of parankylosaurs also fall below the 10 mm threshold for nodosaurids (*sensu* Cross *et al.* 2025). Isolated teeth from South America should be defined taxonomically with caution, because there are no discerning dental features distinguishing a parankylosaurian from the other ankylosaur clades.

Cedarpelta has been resolved variously as an early diverging ankylosaurid (Arbour and Currie 2016), a nodosaurid (Vickaryous *et al.* 2004), or an early diverging ankylosaur (Raven *et al.* 2023). A crucial taxon for understanding the evolution of ankylosaurids, *Cedarpelta* is potentially the oldest ankylosaurid ankylosaur in North America, and may or may not be an ancestor to all other ankylosaurids found in the Campanian–Maastrichtian of North America (Arbour and Currie 2016, Arbour *et al.* 2016). *Cedarpelta* is found slightly below the Aptian–Albian boundary (Suarez *et al.* 2023), with the next oldest Laramidian ankylosaurid represented from skeletal material being *Euoplocephalus* from the Campanian of Canada (Oldman Formation). *Cedarpelta* did not plot in proximity to the shamosaurine ankylosaurids (*Gobisaurus* and *Shamosaurus*) or within the larger Ankylosauridae in any of our phylogenetic analyses. The single *Cedarpelta* tooth studied here was only partly erupted and could not be included in the geometric morphometric outline analyses; however, crown height falls within the range of overlap between nodosaurids and ankylosaurids, but the tooth is larger than most ankylosaurid and basal ankylosaur teeth (CH = 8.33 mm; ankylosaurid mean, 6.49 mm). The tooth does not have a basal cingulum or fluting, suggesting, but not confirming, affinities with Polacanthidae or basal Ankylosauria, rather than Panoplosauridae or Ankylosauridae as suggested by Cross *et al.* (2025). Carpenter *et al.* (2008) suggested that *Cedarpelta* could be a shamosaurine ankylosaurid, like *Gobisaurus* and *Shamosaurus* from Asia, whereas the ankylosaurids in this study belong to the ankylosaurid subclade Ankylosaurinae. *Gobisaurus* has large teeth, with a CBL of 9.5 mm and a CH of 11 mm (Vickaryous *et al.* 2001), larger than what was observed for all ankylosaurine ankylosaurids. The large size of *Gobisaurus* teeth suggests that shamosaurine ankylosaurid tooth size and morphology might differ from those of ankylosaurine ankylosaurids. *Gobisaurus* and *Cedarpelta* have long nodosaurid-like snouts rather than the shorter, wider snouts of ankylosaurine ankylosaurids (Carpenter *et al.* 2001, Vickaryous *et al.* 2001). Their large tooth size relative to ankylosaurids, in combination with a long, narrow snout, might suggest dietary convergence with nodosaurids in shamosaurine ankylosaurids. Small ankylosaurid tooth size might be more representative of ankylosaurines, with larger tooth sizes in shamosaurines and basal ankylosaurids. Cross *et al.* (2025) propose that teeth >10 mm CH and/or CBL are nodosaurid (*sensu* Coombs 1978); however, Asian shamosaurine ankylosaurid teeth exceed that size. We propose, in Late Cretaceous Asia specifically, that teeth >10 mm CH and/or CBL size could be from shamosaurine ankylosaurids. Despite similarities to shamosaurine ankylosaurids, *Cedarpelta* falls outside of Ankylosauridae in all our analyses, suggesting a nodosaurid affinity.

Jakapil has been used to suggest a South American clade of thyreophorans, distinct from Parankylosauria (Riguetti *et al.* 2022a). In most of our phylogenetic analyses, *Jakapil* plots near nodosaurids (*sensu* Coombs 1978) and taxa considered parankylosaurian. Riguetti *et al.* (2022a) suggest that *Jakapil* is the continuation of a 'basal thyreophoran' lineage; however, none of our phylogenetic analyses supports that hypothesis either. All our analyses, except one, plot *Jakapil* within Ankylosauria. Analysis D plots *Jakapil* as an early stegosaur. Our morphometric analyses of both maxillary and dentary teeth place *Jakapil* in morphospace occupied by several ornithischian clades, including Stegosauria, Ankylosauridae, and Nodosauridae. *Jakapil* does not present any tooth morphology that either supports or refutes the potential new South American thyreophoran clade.

Peloroplites was initially considered a large nodosaurid ankylosaur by Carpenter *et al.* (2008), but Raven *et al.* (2023) recovered it as a polacanthid. Raven *et al.* (2023) found four unambiguous synapomorphies for Polacanthidae and one for Panoplosauridae, but only one of the four polacanthid synapomorphies is present in *Peloroplites* because of missing data, and the sole panoplosaurid synapomorphy is also missing. As such, this leaves only one character of the scapulocoracoid (the presence of the ventral process at the posteroventral margin of the glenoid, character 192 of Raven *et al.* 2023) present as the feature identifying *Peloroplites* as polacanthid in the dataset from Raven *et al.* (2023). *Peloroplites* jumps between clades in our various phylogenetic analyses, making it difficult to resolve with only these data. In the morphometric analyses and size comparisons presented here and in the study by Cross *et al.* (2025), *Peloroplites* plots far from Polacanthidae and shows similarities to Panoplosauridae. The *Peloroplites* tooth is more than double the CH and CBL size of all other polacanthid specimens in the dataset of Cross *et al.* (2025). Within both traditional morphometrics and geometric morphometrics, the tooth shape of *Peloroplites* plots on the complete opposite side of the PC1 and LD 1 axes to the rest of Polacanthidae (e.g. Fig. 4D). Considering only dental features, our morphometric results strongly suggest that *Peloroplites* is more likely to be a panoplosaurid ankylosaur, rather than a polacanthid ankylosaur. Alternatively, it is possible that *Peloroplites* is a polacanthid that evolved a specialized dentition reflecting its much larger body size in comparison to all other polacanthids.

Priconodon is an Appalachian taxon, and there is very little Appalachian dinosaur material. In this case, using tooth morphology *Priconodon* is confirmed as a nodosaurid taxon (*sensu* Coombs 1978), with Struthiosauridae being a potential Raven *et al.* (2023) clade identification. Given the paleogeography of Appalachia, it is possible that struthiosaurids might have migrated from Europe and been present in North America. No ankylosaurid ankylosaur material has been recovered from Appalachia until the Maastrichtian (Brownstein 2018).

CONCLUSION

A combined approach of tooth morphometrics and phylogenetic analyses provides insight into the clade associations of ankylosaur taxa with ambiguous taxonomic designations. We develop new dental characters for phylogenetic analyses that accurately represent the morphology present in the clade and have some association with phylogeny. Geometric morphometric analyses allow for the study of shape characteristics that can be phylogenetically relevant yet are difficult to describe using discrete characters in phylogenetic analyses, providing additional evidence to support placement of taxa in these analyses. Methodologies pairing geometric morphometrics with phylogenetic analyses could potentially be applied to other clades for improved phylogenetic clarity.

Resolution and consensus of phylogenetic relationships is necessary for understanding the palaeoecology and palaeobiogeography of ancient organisms. Among ankylosaurs, nodosaurids are found more often in marine/brackish environments, indicating potential different habitat preferences to Ankylosauridae (Arbour *et al.* 2016). This environmental association is useful only if the taxonomic data used in the statistical analysis are grounded with high support. Within this study, we showed that combining morphological and phylogenetic data improved taxonomic assignment for rogue taxa, including *Aletopelta* and *Borealopelta*, which are more strongly supported as nodosaurids. Placing these two taxa within Nodosauridae allows for a stronger association of this ankylosaur clade to marine/brackish environments.

Dental morphometric analyses are useful for finding likely clade associations for taxa described primarily or solely on tooth material. The tooth morphometric identification of *Priconodon* as nodosaurid supports the interpretation that there is no ankylosaurid material from Appalachia prior to the Maastrichtian (*sensu* Brownstein 2018). This insight into Cretaceous terrestrial Appalachian fossil material is crucial for understanding the palaeobiogeography and phylogenetic relationships of North American taxa. Combined morphometric and phylogenetic analyses have the potential to provide better phylogenetic resolution of taxa with meagre material.

CONFLICT OF INTEREST

None declared.

SUPPLEMENTARY DATA

Supplementary data is available at *Zoological Journal of the Linnean Society* online.

FUNDING

Funding for this project was provided by a Dinosaur Research Institute Student Research Grant and a Canadian Museum of Nature Visiting Student Grant to EGC. VMA is funded by a Natural Sciences and Engineering Research Council of Canada Discovery Grant (RGPIN-2020-04012) and Discovery Launch Supplement (DGECR-2020-00149).

DATA AVAILABILITY

All data generated or analysed during this study are provided in full within the published article and its supporting information.

REFERENCES

Agnolín FL, Rozadilla S, Marsà JG *et al.* New remains of the armored dinosaur *Patagopelta cristata* Riguetti *et al.* 2022 (Ornithischia, Parankylosauria) from the Late Cretaceous of Patagonia, Argentina. *Historical Biology* 2026;1–64.

Altekar GS, Dwarkadas S, Huelsenbeck JP *et al.* Parallel metropolis-coupled Markov chain Monte Carlo for Bayesian phylogenetic inference. *Bioinformatics (Oxford, England)* 2004;**20**:407–15.

Álvarez Nogueira RL, Agnolín F, Sebastián R *et al.* Ankylosaurian remains from a new Campanian–Maastrichtian locality in Northern Patagonia, Argentina. *Alcheringa: An Australasian Journal of Palaeontology* 2025;**49**:69–78.

Arbour VM, Currie PJ. *Euoplocephalus tutus* and the diversity of ankylosaurid dinosaurs in the Late Cretaceous of Alberta, Canada, and Montana, USA. *PLoS One* 2013;**8**:e62421.

Arbour VM, Currie PJ. Systematics, phylogeny and palaeobiogeography of the ankylosaurid dinosaurs. *Journal of Systematic Palaeontology* 2016;**14**:385–444.

Arbour VM, Currie PJ, Badamgarav D. The ankylosaurid dinosaurs of the Upper Cretaceous Baruungoyot and Nemegt formations of Mongolia. *Zoological Journal of the Linnean Society* 2014;**172**:631–52.

Arbour VM, Zanno LE, Gates T. Ankylosaurian dinosaur palaeoenvironmental associations were influenced by extirpation, sea-level fluctuation, and geodispersal. *Palaeogeography, Palaeoclimatology, Palaeoecology* 2016;**449**:289–99.

Bapst DW. paleotree: an R package for paleontological and phylogenetic analyses of evolution. *Methods in Ecology and Evolution* 2012;**3**:803–7.

Bapst DW. Assessing the effect of time-scaling methods on phylogeny-based analyses in the fossil record. *Paleobiology* 2014;**40**:331–51.

Bapst DW, Hopkins MJ. Comparing *cal3* and other a posteriori time-scaling approaches in a case study with the pterocephaliid trilobites. *Paleobiology* 2017;**43**:49–67.

Bell MA, Lloyd GT. strap: an R package for plotting phylogenies against stratigraphy and assessing their stratigraphic congruence. *Palaeontology* 2015;**58**:379–89.

Brown CM, Henderson DM, Vinther J *et al.* An exceptionally preserved three-dimensional armored dinosaur reveals insights into coloration and Cretaceous predator-prey dynamics. *Current Biology: CB* 2017;**27**:2514–21.e3. e2513.

Brownstein CD. The biogeography and ecology of the Cretaceous non-avian dinosaurs of Appalachia. *Palaeontologia Electronica* 2018;21.1.5A;1–56.

Burns ME. Intraspecific variation in the armoured dinosaurs (Dinosauria: Ankylosauria). D. Phil Thesis, University of Alberta, 2015.

Carpenter K. Ankylosaur systematics: example using *Panoplosaurus* and *Edmontonia* (Ankylosauria: Nodosauridae). In: K Carpenter, PJ Currie (eds.), *Dinosaur Systematics: Approaches and Perspectives*. Cambridge, UK: Cambridge University Press, 1990, 281–98.

Carpenter K, Bartlett J, Bird J *et al.* Ankylosaurs from the Price River quarries, Cedar Mountain Formation (Lower Cretaceous), East-Central Utah. *Journal of Vertebrate Paleontology* 2008;**28**:1089–101.

Carpenter K, Breithaupt B. Latest cretaceous occurrence of nodosaurid ankylosaurs (Dinosauria, Ornithischia) in Western North America and the gradual extinction of the dinosaurs. *Journal of Vertebrate Paleontology* 1986;**6**:251–7.

Carpenter K, Kirkland JI. Review of Lower and Middle Cretaceous ankylosaurs from North America. *New Mexico Museum of Natural History and Science Bulletin* 1998;**14**:249–70.

Carpenter K, Kirkland J, Burge D, *et al.* Disarticulated skull of a new primitive ankylosaurid from the Lower Cretaceous of Eastern Utah. In: Carpenter K (ed.), *The Armoured Dinosaurs*. Bloomington, Indiana, USA: Indiana University Press, 2001, 211–37.

Chure D, Britt BB, Whitlock JA *et al.* First complete sauropod dinosaur skull from the Cretaceous of the Americas and the evolution of sauropod dentition. *Die Naturwissenschaften* 2010;**97**:379–91.

Coombs WP. The families of the ornithischian dinosaur order Ankylosauria. *Palaeontology* 1978;**21**:1–33.

Coombs WP. Teeth and taxonomy in ankylosaurs. In: K Carpenter, PJ Currie (eds.), *Dinosaur Systematics: Approaches and Perspectives*. Cambridge, UK: Cambridge University Press, 1990, 269–80.

Coombs WP, Deméré TA. A Late Cretaceous nodosaurid ankylosaur (Dinosauria: Ornithischia) from marine sediments of Coastal California. *Journal of Paleontology* 1996;**70**:311–26.

Coombs W, Maryańska T. Ankylosauria. In: DB Weishampel, P Dodson, H Osmólska (eds.), *The Dinosauria*. Berkeley, California, USA: University of California Press, 1990, 456–83.

Cross E, Fraass AJ, Arbour VM. Taxonomic utility of isolated ankylosaurian dinosaur teeth using traditional and geometric morphometrics with implications for ankylosaur paleoecology. *Journal of Paleontology* 2025;**99**:441–57.

Fonseca A, Reid I, Venner A *et al.* A comprehensive phylogenetic analysis on early ornithischian evolution. *Journal of Systematic Palaeontology* 2024;**22**:2346577.

Ford T, Kirkland J. Carlsbad ankylosaur (Ornithischia, Ankylosauria): an ankylosaurid and not a nodosaurid. In: Carpenter K (ed.), *The Armored Dinosaurs*. Bloomington, Indiana, USA: Indiana University Press, 2001, 239–60.

Galton PM. Armored dinosaurs (Ornithischia: Ankylosauria) from the Middle and Upper Jurassic of England. *Geobios* 1980;**13**:825–37.

Galton PM. Armored dinosaurs (Ornithischia: Ankylosauria) from the Middle and Upper Jurassic of Europe. *Palaeontographica, Abteilung A* 1983;**182**:1–25.

Goloboff PA, Morales ME. TNT version 1.6, with a graphical interface for MacOS and Linux, including new routines in parallel. *Cladistics: The International Journal of the Willi Hennig Society* 2023;**39**:144–53.

Gulbranson EL, Rasbury ET, Ludvigson GA *et al.* U–Pb Geochronology and stable isotope geochemistry of terrestrial carbonates, Lower Cretaceous Cedar Mountain Formation, Utah: implications for synchronicity of terrestrial and marine carbon isotope excursions. *Geosciences* 2022;**12**:346.

Harrison LB, Larsson HC. Among-character rate variation distributions in phylogenetic analysis of discrete morphological characters. *Systematic Biology* 2015;**64**:307–24.

Huxley TH. IV.—On *Acanthopholis horridus*, a new reptile from the Chalk-marl. *Geological Magazine* 1867;**4**:65–7.

Leahey LG, Molnar RE, Carpenter K *et al.* Cranial osteology of the ankylosaurian dinosaur formerly known as *Minmi* sp. (Ornithischia: Thyreophora) from the Lower Cretaceous Allaru Mudstone of Richmond, Queensland, Australia. *PeerJ* 2015;**3**:e1475.

Lelièvre PG, Grey M. JMorph: software for performing rapid morphometric measurements on digital images of fossil assemblages. *Computers & Geosciences* 2017;**105**:120–8.

Lomax DR, Tamura N, Hartman S *et al. Dinosaurs of the British Isles*. Rochdale, UK: Siri Scientific Press, 2014.

Lull RS. Systematic paleontology of the Lower Cretaceous deposits of Maryland. *Maryland Geological Survey, Lower Cretaceous* 1911;183–211.

Lydekker R. On the jaw of a new carnivorous dinosaur from the Oxford Clay of Peterborough. *Quarterly Journal of the Geological Society of London* 1893;**49**:284–7.

Maddison WP, Maddison DR. Mesquite: a modular system for evolutionary analysis. Version 3.81, 2023. https://www.mesquiteproject.org (29 September 2025, date last accessed).

Maidment S, Ouarhache D, Ech-Charay K *et al.* Extreme armour in the world's oldest ankylosaur. *Nature* 2025;**647**:121–6.

Marsh OC. Notice of a new genus of Sauropoda and other new dinosaurs from the Potomac Formation. *American Journal of Science* 1888;**s3-35**:89–94.

Matzke NJ, Wright A. Inferring node dates from tip dates in fossil Canidae: the importance of tree priors. *Biology Letters* 2016;**12**:20160328.

Molnar RE. Preliminary report on a new ankylosaur from the Early Cretaceous of Queensland, Australia. *Memoirs of the Queensland Museum* 1996;**39**:653–68.

Ősi A. The European ankylosaur record: a review. *Hantkeniana* 2015;**10**:89–106.

Pereda-Suberbiola XP, Barrett PM. A systematic review of ankylosaurian dinosaur remains from the Albian-Cenomanian of England. *Special Papers in Palaeontology* 1999;**60**:177–208.

R Core Team. *R: a Language and Environment for Statistical Computing*. Vienna, Austria: R Foundation for Statistical Computing, 2021.

Raven TJ, Barrett PM, Joyce CB *et al.* The phylogenetic relationships and evolutionary history of the armoured dinosaurs (Ornithischia: Thyreophora). *Journal of Systematic Palaeontology* 2023;**21**:2205433.

Revell LJ. phytools 2.0: an updated R ecosystem for phylogenetic comparative methods (and other things). *PeerJ* 2024;**12**:e16505.

Riguetti FJ, Apesteguía S, Pereda-Suberbiola X. A new Cretaceous thyreophoran from Patagonia supports a South American lineage of armoured dinosaurs. *Scientific Reports* 2022a;**12**:11621.

Riguetti F, Pereda-Suberbiola X, Ponce D *et al.* A new small-bodied ankylosaurian dinosaur from the Upper Cretaceous of North Patagonia (Río Negro Province, Argentina). *Journal of Systematic Palaeontology* 2022b;**20**:2137441.

Ronquist F, Teslenko M, van der Mark P *et al.* MRBAYES 3.2: efficient Bayesian phylogenetic inference and model selection across a large model space. *Systematic Biology* 2012;**61**:539–42.

Salgado L, Gasparini Z. Reappraisal of an ankylosaurian dinosaur from the Upper Cretaceous of James Ross Island (Antarctica). *Geodiversitas* 2006;**28**:119–35.

Seeley HG. *Index to the Fossil Remains of Aves, Ornithosauria, and Reptilia from the Secondary Strata arranged in the Woodwardian Museum of the University of Cambridge*. Cambridge: Deighton, Bell and Co., 1869, 144 pp.

Seeley HG. On the maxillary bone of a new dinosaur (*Priodontognathus phillipsii*), contained in the Woodwardian Museum of the University of Cambridge. *Quarterly Journal of the Geological Society of London* 1875;**31**:439–43.

Sereno PC, Zhimin D. The skull of the basal stegosaur *Huayangosaurus taibaii* and a cladistic diagnosis of Stegosauria. *Journal of Vertebrate Paleontology* 1992;**12**:318–43.

Soto-Acuña S, Vargas AO, Kaluza J *et al.* Bizarre tail weaponry in a transitional ankylosaur from subantarctic Chile. *Nature* 2021;**600**:259–63.

Soto-Acuña S, Vargas A, Kaluza J. A new look at the first dinosaur discovered in Antarctica: reappraisal of *Antarctopelta oliveroi* (Ankylosauria: Parankylosauria). *Advances in Polar Science* 2024;**35**:78–107.

Suarez MB, Al Suwaidi A, Montgomery EH *et al.* New geochronological age constraint and chemostratigraphy for Aptian lacustrine strata, Cedar Mountain Formation, Utah. *Geochemistry, Geophysics, Geosystems* 2023;**24**:e2023GC011014.

Thompson RS, Parish JC, Maidment SCR *et al.* Phylogeny of the ankylosaurian dinosaurs (Ornithischia: Thyreophora). *Journal of Systematic Palaeontology* 2012;**10**:301–12.

Vickaryous MK, Maryańska T, Weishampel DB. Ankylosauria. In: DB Weishampel, P Dodson, H Osmólska (eds.), *The Dinosauria*, 2nd edn. Berkeley, CA: University of California Press, 2004, 363–92.

Vickaryous MK, Russell AP, Currie PJ *et al.* A new ankylosaurid (Dinosauria: Ankylosauria) from the Lower Cretaceous of China, with comments on ankylosaurian relationships. *Canadian Journal of Earth Sciences* 2001;**38**:1767–80.